Climate, wind energy, and CO_2 emissions from energy production in Denmark[☆]

Federico Carlini [a], Bent Jesper Christensen [b,c,*], Nabanita Datta Gupta [d],
Paolo Santucci de Magistris [a,b]

[a] *LUISS University, Department of Economics and Finance, Viale Romania 32, 00197 Roma, Italy*
[b] *CREATES, Aarhus University, Department of Economics and Business Economics, Fuglesangs Allé 4, DK-8210 Aarhus V, Denmark*
[c] *Dale T. Mortensen Center, Aarhus University, Department of Economics and Business Economics, Fuglesangs Allé 4, DK-8210 Aarhus V, Denmark*
[d] *Aarhus University, Department of Economics and Business Economics, Fuglesangs Allé 4, DK-8210 Aarhus V, Denmark*

A B S T R A C T

The dynamic relation between CO_2 emissions and wind energy in Denmark is analyzed using a fractional cointegration approach, extended to accommodate covariates. The impact of climate and forces of demand on the potential of wind power production for emissions abatement is investigated. Emissions decline as temperature increases. Wind power production increases with precipitation and North Atlantic oscillations. Aggregate output matters for emissions in a manner consistent with an environmental Kuznets curve (EKC). Accounting for a seasonal trend, our main estimate of marginal CO_2 emissions avoided (MEA) per MWh of wind energy produced is 0.16 tonnes, based on impulse responses. This estimate of the abatement potential of wind power is lower than values reported in the literature, but statistically significant, and robust to including climate and EKC variables. MEA is reduced by about one third by treating electricity prices as endogenous, and by one quarter by including emissions from combustion of biomass. However, formal exogeneity tests indicate that the main MEA estimate is not inflated due to left-out general equilibrium effects. Without covariates, estimated MEA is 0.07, and insignificant.

1. Introduction

The global warming and climate change observed over recent decades are mainly caused by greenhouse gas (GHG) emissions (Stocker et al., 2013). The largest component of GHG emissions is carbon dioxide (CO_2) emissions,[1] stemming mainly from the combustion of fossil fuels such as coal, oil, and natural gas for the purpose of energy generation. In an attempt to address the challenges of climate change, the 2015 Paris Agreement joined by most countries of the world advocates limiting the global temperature rise to 1.5 °C above pre-industrial levels. According to the Intergovernmental Panel on Climate Change (IPCC, 2019), this will require cutting global CO_2 emissions to net zero by 2050. One of the policy tools toward meeting these demands, as part of the rising combat against global warming, is the adoption of clean energy sources, such as wind and solar, as replacements of fossil fuels. It appears obvious that clean energy adoption should reduce emissions, as would be implied by a basic engineering analysis, based on a displacement or dispatch approach. Nevertheless, obtaining a precise, quantitative measure of the causal effect of clean energy adoption on emissions is hampered by a number of factors, relating to climate as well as supply and demand conditions.

In this paper, we conduct a dynamic econometric analysis to assess the potential role of the adoption of wind energy production for CO_2 emissions abatement in Denmark. Wind energy is already important in Denmark, covering 47% of gross electricity consumption as of 2019. In the analysis, we account for covariates, including a seasonal trend, as well as controls for climate and supply and demand conditions.

We show that this has a strong impact on the results. First, local climate conditions, including temperature and weather patterns, can impact the relation between emissions and abatement efforts in several ways. Temperature changes matter directly for demand for heating and cooling (air conditioning), and together with climatic parameters such as turbulence, oscillations, precipitation, sunshine, and air density determines the efficiency of wind energy generation. Second, changes in aggregate demand clearly impact emissions. Furthermore, changes in wind power production can shift power supply, and thus output (electricity) prices, as well as demand for fossil fuels, and thereby input (fuel) prices in conventional power production. Third, trends in series imply a risk of finding a spurious effect, and any potential causal effect should be allowed sufficient time to set in, hence calling for a dynamic analysis. Responses to price changes are potential endogenous mechanisms in the system, with feedback on wind production itself. Further endogeneity issues arise because wind adoption decisions can be direct responses to changes in emissions. The desired causal effect is the full effect of wind adoption on emissions, accounting for these equilibrium effects, and cannot be estimated by OLS regression of emissions on wind production, or any engineering method.

We include a seasonal trend, temperature, other climate variables, and variables capturing supply and demand conditions, in a monthly frequency analysis of the dynamic relation between CO_2 emissions from total energy production and wind energy produced in Denmark over the period January, 2005, through December, 2019. Based on a fractional cointegration analysis, our focus is on long-run persistence and the dynamic relation in the bivariate system. Previous literature has studied the relation between CO_2 emissions and wind energy using regression methods over shorter periods, controlling for temperature and demand. Accordingly, we extend the fractional cointegration model to account for explanatory variables, including climate indicators, demand, trend, and seasonality. In addition, we consider further extended systems, including input (fossil fuel) and output (electricity) prices as potentially endogenous variables characterizing supply and demand conditions. Prices matter for the incentive to substitute wind energy for conventional power production, and at the same time react to consumer and producer supply and demand.

The extension to account for climate variables is important. Local climatic conditions clearly impact the amount of CO_2 emitted, as well as the relation between emissions and wind power production. Temperature matters both for energy demand, with a direct effect on emissions unrelated to wind energy, and for efficiency in wind generation. The effect of temperature on demand stems mainly from demand for heating and cooling. Global warming in the Northern hemisphere, improved housing materials, and better insulation have reduced heating demand and increased demand for air conditioning (Stocker et al., 2013), with a negative net effect on energy demand in cold countries. In Denmark, most heating is generated from the burning of coal, natural gas, and biomass, with only a small fraction covered via by-products (excess heat) from electricity production, implying a negative direct demand effect of higher temperature on emissions. The efficiency effect works in the opposite direction, because higher temperature makes the air less dense, hence reducing the efficiency of the thermodynamic cycle used to drive turbines (Cullen, 2013). The total impact of temperature on emissions is a combination of the direct demand and the indirect efficiency effects.

Wind generation is affected by other local climatic conditions, too, including turbulence, oscillations, precipitation, and sunshine. On stormy days, more wind power is generated, while on calm, sunny days, the opposite occurs, implying that a mix of wind and solar energy can complement each other (Jacobson and Delucchi, 2011). Similarly, ice and snow can damage or slow down wind turbines (Pieralli et al., 2015). We obtain monthly observations on temperature, precipitation, and sunshine hours from the Danish Meteorological Institute (DMI), and on the North Atlantic Oscillation Index (NAOI) from the Climate Prediction Center of the US Government National Weather Service.

NAOI captures atmospheric variability patterns affecting Northern Europe, oscillating between positive and negative values associated with stronger jet stream and decreased storminess, respectively. It depends on surface sea-level pressure differences between the Southern and Northern Atlantic regions, and is highly correlated with other measures of atmospheric circulation, such as dp(abs)24, which is the interdiurnal pressure-variability index, and with wind speed and storminess (Hanna et al., 2008).

We include the climate variables among the predetermined explanatory variables in the analysis of the relation between CO_2 emissions and wind energy. The assumption here is that while local climatic conditions affect local emissions, they are caused by global climatic conditions, including global emissions, rather than by local emissions. For example, local temperature is not affected by local emissions, but rather by accumulated global emissions (Leduc et al., 2016). Further, as an additional indicator for demand, beside temperature, we include industrial production, a proxy for aggregate output. The monthly industrial production index is obtained from Eurostat. By adopting a quadratic specification, an environmental Kuznets curve (EKC) is accommodated, the hypothesis being that emissions increase at a decreasing rate with economic development, here output (Grossman and Krueger, 1995; Holtz-Eakin and Selden, 1995).

Our empirical results indicate a significantly negative relation between CO_2 emissions and wind energy production. We calculate impulse response functions, marginal emissions avoided (MEA) per MWh of energy produced by wind, and long-run forecasts of emissions and wind production. From the results, temperature matters more for emissions in its capacity as a driver of demand for heating than through its effect on generation efficiency, as emissions decline with rising temperature. Wind power production increases with precipitation and North Atlantic oscillations, both of which signal stormy weather. Aggregate output matters for emissions in a manner consistent with the EKC. Accounting for a seasonal trend, MEA is estimated at 0.16 tonnes of CO_2 emissions avoided per MWh of wind energy produced, based on impulse responses, which include the long-run equilibrium relation, as well as short-run dynamics. This estimate of the abatement potential of wind power is lower than values reported in the literature, but statistically significant, and robust to including climate and EKC variables. Estimated MEA is reduced further, by about one third, by accounting for general equilibrium effects operating via electricity prices, and by one quarter by including emissions from combustion of biomass. On the other hand, including fuel prices as exogenous or endogenous variables can increase MEA by one quarter, to about 0.20. Formal exogeneity tests indicate that our main MEA estimate, at 0.16, is not inflated due to left-out general equilibrium effects. Without covariates, estimated MEA is 0.07, and insignificant.

The paper is laid out as follows. Section 2 discusses the literature, how our work relates to this, and our contributions. Section 3 presents the fractional cointegration model. Section 4 introduces the data and provides a preliminary regression analysis. Section 5 discusses the main empirical analysis. Section 6 concludes. Additional results are collected in Appendix A and Appendix B.

2. Relation to literature

An early study is Cullen (2013), regressing conventional (coal, natural gas, nuclear, etc.) power production on wind energy production, temperature, and demand, using data from the Electricity Reliability Council of Texas (ERCOT) grid over the period 2005–2007. MEA is derived in terms of a partial derivative, multiplying emissions factors onto conventional production offset by wind, and estimated at .43.[2]

---

[2] Henceforth, MEA is stated in tCO_2/MWh, i.e., tonnes of CO_2 emissions avoided per MWh of energy produced by wind.

Similarly using ERCOT data, Novan (2015) corrects for potential endogeneity of wind production in 2SLS regressions.[3] Using data for 2011 from Ireland, Wheatley (2013) accounts for serial correlation by taking first differences of series, as well as allowing for ARMA(1,1) errors. Other studies for Ireland address dynamics by allowing for AR(1) residuals (Di Cosmo and Valeri, 2018a) or wind forecasting errors (O'Mahoney et al., 2018), or by reporting Newey and West (1987) standard errors (Oliveira et al., 2019).[4]

In relation to the regression literature, we similarly compute emissions by applying emissions factors to conventional production, derive MEA in terms of partial derivatives, and control for temperature and demand. Instead of high-frequency (e.g., 15-minute in Cullen, 2013) panel observations on production at the individual generator level over a short calendar period, we conduct a long-run monthly-frequency analysis. We handle dynamics much more generally than in the regression studies, allowing for potential long memory and error correction. Long memory refers to the feature that emissions and wind energy are strongly persistent, more so than a stationary ARMA process, as we document. Cointegration and error correction indicate that these variables (along with prices, in the extended models) move together in the long run. Rather than correcting for endogeneity of wind energy in the emissions equation using 2SLS, we use cointegration to separate causal from spurious relations, and test for exogeneity in the system analysis. Here, although the notion of spurious relations is usually associated with apparent relations (due to nonsense regression results) among unit root processes that are in fact unrelated, the desired (non-spurious) case being that they move together in the long run, i.e., cointegrate to a short-memory process, we consider the similar notion for the stationary long-memory (fractionally integrated) series in our data.[5]

Our work is most closely related to that of Christensen et al. (2021) (henceforth CDS), who introduce the fractional cointegration approach to the relation between the de-seasonalized CO_2 and wind energy series, document a structural break around 2005, derive MEA, and provide forecasts of both variables through 2050. The structural break coincides in time with the implementation of the European Union Emissions Trading Scheme (EU ETS) and the Kyoto Protocol, as well as announcements by policy makers about further investments in wind power, and so may well be policy driven, with faster rate of reduction in emissions and increase in wind power after 2005 than before. Therefore, in the present study, we use 2005 as the starting year of our analysis data set.

We offer a number of incremental contributions on the methodological and data sides, relative to CDS. First, in terms of the econometric model, we include predetermined explanatory variables in the fractional cointegration analysis. These are exploited in several ways that matter for the application: (i) We include climate variables, which is important for the assessment of the potential of wind for emissions abatement; (ii) by including seasonality terms among the predetermined variables, the corresponding adjustments are estimated along with other model parameters; (iii) motivated by the regression literature, we control for demand. In contrast, CDS pre-adjust data for seasonality before estimation, and include climate variables and demand only in a preliminary regression analysis, not in the fractional cointegration analysis. Further, we account for potentially endogenous effects of supply and demand operating via prices of inputs (fuels) and output (electricity) in power production. In terms of data, we add about two years of observations, as our series are updated through December, 2019, as opposed to November, 2017, in CDS. Moreover, we include emissions from combustion of waste, and in some of our specifications

from combustion of biomass, too, in our emissions measure, in addition to the CO_2 emissions from combustion of fossil fuels for energy production considered in CDS. Some of our work is organized as a sensitivity analysis, in order to assess the incremental value of each of these contributions.

Combustion of waste constitutes a considerable portion of conventional power production in Denmark, alongside combustion of fossil fuels, and hence the importance of adding emissions from waste burning to our measure of CO_2, relative to CDS. A further fuel combusted for energy generation is biomass. The role of waste and biomass burning for emissions and energy production has been studied by Hernandez et al. (2019),[6] using a dynamic displacement approach, rather than an econometric approach. A displacement approach assumes that the proposed technology (in our case, wind power) replaces an equal amount of power generated by the existing system. Static versions of the approach have been used by wind industry associations, governments, and international organizations, e.g., the European Wind Energy Association (EWEA, Corbetta et al., 2015), the Global Wind Energy Council (GWEC, 2016), and the Sustainable Energy Authority of Ireland (SEAI, 2019). Hernandez et al. (2019) suggest a version with dynamic displacement emission factors (comparable to MEA), updated periodically according to anticipated changes in the future generation portfolio. In contrast, our econometric approach uses the observed time-varying energy mix to imply the emissions series, then estimates the impact of wind share on this from historical data, in effect identifying the marginal generator replaced from actual observations. Further, our estimated effects are accompanied by significance levels and hypothesis tests, and the approach accommodates potential endogeneity, such as prices reacting to adoption decisions, none of which is available in the displacement approach. We compare results with and without waste and biomass in the emissions measure in our econometric analysis.

Some studies have used a dispatch model, an engineering based refinement of the displacement approach using detailed information on the structure of the power system and applicable, e.g., for counterfactual scenario analysis. Technologies (generators) are ranked in a production stack according to marginal cost, and unit commitment, dispatch, and power flow selected to minimize cost of meeting assumed demand, subject to system constraints, including generator capacities, network constraints, cost and emission effects of start-up, shut-down, part-load operation, cycling, ramping, etc. PLEXOS, a commercial power market simulation software solving the unit commitment and dispatch problems by mixed integer programming, has been used by governments, e.g., the U.S. Department of Energy, the National Renewable Energy Laboratory (NREL, 2013), for the Western interconnection, consisting of the United States, Canada, and Mexico, and SEAI for Ireland (Clancy and Gaffney, 2014). Using similar software, Valentino et al. (2012) find that the adoption of wind can lead to reduction of emissions in Illinois.

In contrast, in our econometric approach, rather than computing the cost-minimizing or otherwise optimizing replacement from assumptions within a dispatch model, we implicitly identify the technology actually replaced through observed responses in emissions to changes in wind generation, potentially reflecting changes over time in climatic and demand conditions, investments, technology, and decision-making behavior. Again, unlike in the engineering approach, our estimates and forecasts are accompanied by assessments of uncertainty and hypothesis testing, accounting for potential endogeneity, so the econometric approach can generate important additional insights.

The bivariate model, with CO_2 emissions and wind power production as dependent variables, allows an analysis of the relation among the two, but potentially suffers from an omitted variable problem, with prices left out. This can lead to endogeneity bias in the estimated

---

[3] Siler-Evans et al. (2012) and Kaffine et al. (2013) are related US studies.

[4] Other regression studies include Amor et al. (2014) for the Ontario grid, and Thomson et al. (2017) for Great Britain.

[5] Thus, we consider the apparent relation among long-memory processes as spurious if they do not move together in the long run, and we show graphically that they do in cases where we detect fractional cointegration.

[6] For biomass, see also Weldemichael and Assefa (2016).

emissions abatement effect of wind, and hence the importance of our extended models, including prices as dependent variables. An increase in wind power production implies lower demand for fossil fuels, and thus potentially a drop in fuel prices, partially offsetting the reduction in fuel demand, and hence mitigating the impact on emissions of the increase in wind power. The upshot is that the general equilibrium impact of wind power production on emissions potentially falls short of the initial estimate that ignores the demand effect, operating via input (fuel) prices. An analogous effect can enter via output (power) prices, too. An increase in the supply of wind power production can replace some conventional production, but can potentially reduce power prices, too, in turn increasing power demand. As power production is increased to meet demand, some of the increase remains conventional, given the generation mix, thus partially offsetting the reduction in conventional production. Again, the impact of wind on emissions is mitigated in equilibrium. The latter effect, through electricity prices, is emphasized by Abrell et al. (2019) in a regression study of wind and solar subsidies in Germany and Spain. Similarly, Amor et al. (2014) and Di Cosmo and Valeri (2018b) regress electricity prices in Ontario and Ireland, respectively, on wind generation, demand, and other controls. In a dynamic context, energy prices behave like commodity prices (Pindyck, 1999, 2001), i.e., neither as random walks (like financial assets) nor independently across time, so a fractional model is natural. Accordingly, we include prices of electricity and fuels in our extended fractional models. Although the above regression studies include electricity prices, previous literature on emissions has not considered fuel prices, and all endogeneity issues are ignored in the engineering (displacement and dispatch) literature.

Our results are consistent with an upward endogeneity bias in the estimated abatement potential of wind energy from leaving out electricity prices, or treating these as exogenous. MEA is reduced by one third when including electricity prices as endogenous variables. In contrast, including fuel prices as endogenous, or both electricity and fuel prices as exogenous variables does not reduce MEA.

3. The model

We examine the relation between the emissions and wind energy production series, allowing for the possibility that they are (fractionally) cointegrated, i.e., that their paths are tied together in a long run equilibrium relation. Further, we investigate the possible dependence of this relation on a number of covariates, including climate and demand variables. To this end, we extend the fractional vector error-correction model (FVECM$_{d,b}$) introduced by Granger (1986) and subsequently studied by Davidson (2002) to accommodate explanatory variables. The extended model, labeled FVECM-X$_{d,b}$, is given by

$$\Delta^d Y_t = \alpha \beta' \Delta^{d-b} L_b Y_t + \sum_{j=1}^{k} \Gamma_j \Delta^d L_c^j Y_t + \varepsilon_t, \quad t = 1, \ldots, T, \tag{1}$$

where $\varepsilon_t \sim N(0, \Sigma)$, $Y_t = Z_t - \mu_t$ contains the deviations between the original p-dimensional data series Z_t and the $p \times 1$ vector μ_t, which determines the dependence of Z_t on a number of explanatory variables. In our base case, $p = 2$, with $Z_t = (E_t, W_t)'$, where E_t and W_t are the emissions and wind energy series, respectively. In most of our work, we measure E_t as the logarithm of CO_2 emissions from energy production, and W_t by a logit transform of the share of wind power in total energy production (see Section 4 for details).

The extension, relative to FVECM$_{d,b}$, is given by μ_t. In our implementation of the FVECM-X$_{d,b}$, we focus on the specification

$$\mu_t = \mu + \zeta_0 t + \zeta_1 \sin(2\pi t/12) + \zeta_2 \cos(2\pi t/12) + \Lambda X_t, \tag{2}$$

where μ is a p-vector of constants capturing the influence of initial values, i.e., non-zero starting points for the first observation on the process (see Nielsen and Shibaev (2018) in the FCVAR$_{d,b}$ context), ζ_i, $i = 0, 1, 2$ are p-vectors of loadings on a set of deterministic terms (linear

trend and seasonals), and Λ is a $p \times q$ matrix of loadings on a $q \times 1$ vector X_t containing the covariates.

In Eq. (1), the term Δ^d is the fractional difference operator,

$$\Delta^d := (1 - L)^d = \sum_{j=0}^{\infty} (-1)^j \binom{d}{j} L^j, \tag{3}$$

with L the (ordinary) lag operator, i.e., $L^j Y_t = Y_{t-j}$, and $L_b := 1 - \Delta^b$ the *fractional lag operator* of Johansen (2008). The long-run dynamics in (1) are governed by the $p \times r$ matrices α and β, $0 \leq r \leq p$. Here, the columns of β are the equilibrium or cointegration vectors, α the speeds of error correction or adjustment to equilibrium, and r the cointegration rank. Short-run dynamics are governed by the $p \times p$ matrices Γ_j, $j = 1, \ldots, k$, and $\Sigma > 0$ is the positive definite covariance matrix of the error terms ε_t. The coefficient $d \geq 0$ determines the order (degree) of long memory or fractional integration of the series Y_t, and b the *cointegration gap*, $0 \leq b \leq d$, i.e., while Y_t is integrated of order d, or $I(d)$, the departure from equilibrium or error-correction term $\beta' Y_t$ is $I(d - b)$. If $d > 0$, the series Y_t exhibit long memory, with autocorrelation functions decaying hyperbolically, as opposed to geometrically, as in the stationary ARMA case (in which $d = 0$). If, in addition, $b > 0$, then the long memory series move together in the long run, in that a linear combination of them, given by the error-correction term, exhibits shorter memory than the original series.

The classic cointegrated VECM model studied in Johansen (1991, 1995) corresponds to the special case $\mu_t = \mu$, $d = b = c = 1$. For $\mu_t = \mu$, but d, b free, the resulting FVECM$_{d,b}$ in (1) is similar to the FVECM$_{d,b}$ of Granger (1986), and the FCVAR$_{d,b}$ proposed by Johansen (2008), with a slight difference arising in the short-run component for $k \geq 1$, as it involves the additional lag operator L_c, where FVECM$_{d,b}$ instead uses the ordinary lag operator, i.e., imposing $c = 1$, and FCVAR$_{d,b}$ uses L_b, i.e., imposing $c = b$. As outlined in Carlini and Santucci de Magistris (2019a), imposing $c = 1$ rather than $c = b$ avoids certain identification problems stemming from an over-specified lag structure. Further identification issues related to the selection of lag length can be avoided by setting c to a suitable finite constant, as noted by Carlini and Santucci de Magistris (2019b), who recommend a value $c = 2$. All three specifications ($c = 1, 2, b$) coincide for $k = 0$ (no short-run component). In the FVECM-X$_{d,b}$, we include the extension involving μ_t from (2), accounting for explanatory variables, and find empirically that $k = 0$ suffices in this case. Furthermore, substantive conclusions are robust to estimation with $k = 1$ and either specification of c.[7]

The parameters of the FCVAR$_{d,b}$ are consistently estimated by maximum likelihood (ML), as shown by Johansen and Nielsen (2012). Carlini and Santucci de Magistris (2019b) adopt an ML procedure for the FVECM$_{d,b}$, and we estimate the parameters of the FVECM-X$_{d,b}$ model by ML, as well. The estimation is carried out in MATLAB, adapting the routine written for FCVAR$_{d,b}$ by Nielsen and Popiel (2018). The asymptotic inference on β, MEA, and the rank test are based on bootstrap, and that on the remaining parameters on asymptotic normality, with estimated standard errors read off the square-roots of the negative diagonal elements of the inverse Hessian at the optimum.

4. Data and preliminary analysis

Our analysis is based on monthly data over the period January 2005 through December 2019. For emissions, we focus on those from energy production. The energy sector is the largest source of CO_2 emissions in Denmark (see the National Inventory Report, Nielsen et al., 2016, p. 82). Furthermore, emissions from energy production is the portion of total emissions that the adoption of wind energy may have an impact on. Thus, we do not consider emissions from transportation,

---

[7] We suppress c in the notation FVECM-X$_{d,b}$, as this is restricted to 1, 2, or b.

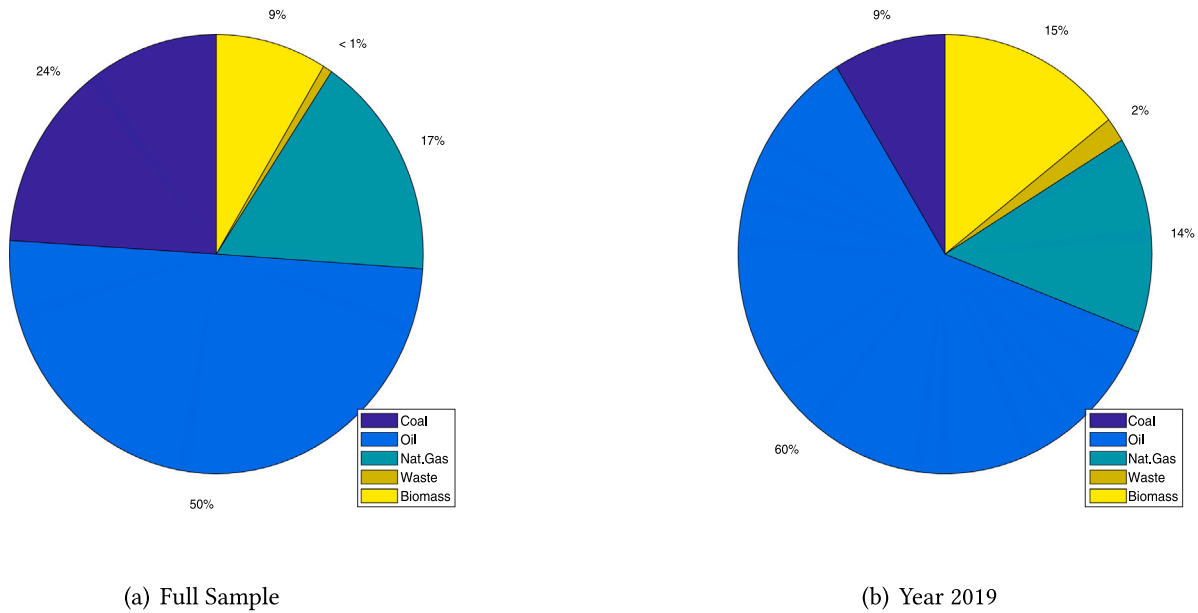(a) Full Sample   (b) Year 2019

Fig. 1. CO_2 emissions composition. The figure reports the composition of CO_2 emissions as average over the full sample 2005–2019 (Exhibit a), and over the last year (Exhibit b).

agriculture, or other sources. We compute total CO_2 emissions from energy production in period t as

$$CO_{2,t} = \sum_{i=1}^{S} C_{i,t} IEF_{i,t}, \qquad (4)$$

where $C_{i,t}$ is consumption of the ith fuel type, and $IEF_{i,t}$ the associated implied emissions factor. In our main analysis, we consider $S = 4$ fuels, namely, coal, oil, natural gas, and waste. In a sensitivity analysis, we include solid biomass, as well, so $S = 5$. Monthly data on $C_{i,t}$ are obtained from the Danish Energy Agency (DEA) under the Ministry for Energy, Utilities and Climate. DEA produces annual and monthly Energy Accounts of the official energy statistics for the country, which include data on energy production, consumption, and emissions.[8] For $IEF_{i,t}$, the EU ETS conducts fuel analysis based on data from all reporting plants to construct IEFs. These are used in Denmark's National Inventory Reports (see Nielsen et al., 2016), prepared annually by the Danish Center for Environment and Energy (DCE), which is responsible for submitting Denmark's national emission inventory under the United Nations Framework Convention on Climate Change (UNFCCC) and the Kyoto Protocol. Average IEF (including the oxygenation factor) over the period is 94.17 kg CO_2 per GJ for coal,[9] 79.49 kg/GJ for residual oil combusted in public electricity and heat generation facilities, 57.381 kg/GJ for natural gas, and 39.06 kg/GJ for non-biodegradable waste burning.

Fig. 1 shows the composition of emissions, corresponding to (4), for the full sample period, as well as for the last year, 2019. Most of the emissions stem from the burning of oil, especially toward the end of the period. The relative weight of emissions from the burning of coal has been reduced over the period, and those from waste and, particularly, biomass increased, with the latter included in the sensitivity analysis, only.[10]

Monthly data on $Prod_t$, production of electricity (net of electricity used in electricity production), and $Wind_t$, electricity production from wind energy, are obtained from DEA. The original source is a

national database known as the 'Stamdataregisteret', which contains information about production for all electricity-producing wind power production facilities. The monthly wind share, or wind penetration, is therefore

$$w_t = \frac{Wind_t}{Prod_t}. \qquad (5)$$

The focus on electricity production is chosen because the data in this case allow isolating the wind share, which is expected to be close to that in total energy production.

From a production function point of view, there should be a fundamental relation between emissions from electricity production, (4), and wind share, (5). Total production is

$$Prod_t = Wind_t + \sum_{i=1}^{S} Prod_{i,t}, \qquad (6)$$

where $Prod_{i,t} = \alpha_{i,t} C_{i,t}$ is production using the ith fuel, for simplicity writing $\alpha_{i,t}$ for the marginal efficiency of the latter. The emissions efficiency (EE) of the ith fuel is $\gamma_{i,t} = IEF_{i,t}/\alpha_{i,t}$, and aggregate and complementary EE (AEE and CEE) are

$$\gamma_t = \sum_{i=1}^{S} \gamma_{i,t}, \qquad \delta_{i,t} = \sum_{j \neq i} \gamma_{j,t}, \qquad (7)$$

where EE = AEE − CEE, for each fuel. Because $C_{i,t} IEF_{i,t} = \gamma_{i,t} Prod_{i,t}$, emissions (4) are

$$CO_{2,t} = \sum_{i=1}^{S} \gamma_{i,t} Prod_{i,t} = \sum_{i=1}^{S} (\gamma_t - \delta_{i,t}) Prod_{i,t}$$

$$= \gamma_t (1 - w_t) Prod_t - \sum_{i=1}^{S} \delta_{i,t} Prod_{i,t}, \qquad (8)$$

where the last equality follows from (5) and (6). By (8), there is a time-varying nonlinear functional relation between $CO_{2,t}$ and w_t. It is this relation that we aim to capture using our econometric approach, including fractional cointegration, allowing for persistence and endogeneity of variables, beyond production function based links.

One implication of (8) is that as wind share approaches unity, emissions approach zero. This is not imposed in our models which, therefore, are not expected to apply for w_t near one, and this is a caveat regarding our long-term forecasts, for which wind share becomes large for positive emissions. Still, with the wind share at 47% in Denmark by

---

[8] https://ens.dk/service/statistik-data-noegletal-og-kort/maanedlig-og-aarlig-energistatistik.

[9] 1 kg CO_2/GJ = 0.0036 tCO_2/MWh.

[10] It is debatable whether biomass should be considered a clean source, as it requires replanting of vegetation, for absorption of CO_2 in the future.

Table 1

Summary statistics. The table reports summary statistics for the monthly data series over the period January, 2005 through December, 2019. ADF regressions include a linear trend, and a number of lagged first differences selected by AIC (maximum 3 lags). In the ADF regressions, CO_2 and industrial production are measured in logarithms, and wind share by the logit transform (10). The Ljung–Box (LB) tests are computed with 6 lags.

Variable	Unit	Mean	Std.Dev.	ADF	p-val	ADF*	p-val	LB	p-val
CO_2	1000 tonnes	3820.7	815.05	−11.059	<0.0010	−6.3626	<0.0010	354.13	0.0000
wind share	Share in energy prod.	0.3285	0.1536	−5.3836	<0.0010	−6.2041	<0.0010	690.70	0.0000
ind	IPI (2010 = 100)	98.594	9.5090	−2.5039	0.3440	−2.4354	0.3776	850.17	0.0000
temp	Degrees °C	8.9239	5.8530	−16.297	<0.0010	−6.8362	<0.0010	466.41	0.0000
precip	mm	64.498	31.279	−6.9294	<0.0010	−9.2570	<0.0010	27.575	0.0001
sunshine	Hours	144.271	81.867	−11.525	<0.0010	−9.4940	<0.0010	375.99	0.0000
NAOI	Index	−0.0399	1.1338	−6.371	<0.0010	−7.5366	<0.0010	34.0421	0.0000
cumul. CO_2	1000 tonnes	377.15	198.41	−1.0663	0.9307	−1.6486	0.7629	986.48	0.0000
cumul. Wind	1000 MhW	65.148	45.728	−0.0292	0.9954	0.5754	0.9990	985.98	0.0000

2019, we assume that our models provide a reasonable approximation over the sample period, and in the not too distant future.

For purposes of empirical estimation, we mostly focus on log emissions,

$$E_t = \log CO_{2,t}, \tag{9}$$

with $CO_{2,t}$ from (4), and

$$W_t = \log\left(\frac{w_t}{1 - w_t}\right), \tag{10}$$

logit of wind share from (5), in our model specifications. Wind share or production mix is preferred over level of wind generation for interpretation and policy purposes. The log transforms in (9) and (10) avoid truncated error distributions. Further, the distribution of changes in emissions depends on the level, and the log transform has a stabilizing effect on this. For comparison, in addition to our main results, based on the log emissions and logit wind share specification, we also report results using raw data on emissions and wind generation, i.e., $CO_{2,t}$ and $Wind_t$. Misspecification tests reject normality of errors in this case.

As an indicator of demand, and to allow for an EKC, aggregate output and its square are included in the model. Industrial production is used as a measure of output, since GDP is not available at monthly frequency. The monthly industrial production index for Denmark is retrieved from Eurostat, with base year 2010. Monthly data on temperature (in °C), precipitation (in mm), and sunshine (in hours) are obtained from DMI historic records (Cappelen, 2018), which have been maintained consistently since 1874 (cf. Cappelen and Jørgensen, 2011). Monthly NAOI levels are obtained from the Climate Prediction Center of the US Government National Weather Service.[11]

Summary statistics are given in Table 1. Sample size is $T = 180$. Wind penetration (5) averages 33% over the period. The Ljung–Box test shows strong serial dependence in all series, so augmented Dickey–Fuller (ADF) regressions are implemented, with CO_2 emissions and industrial production (*ind*) measured in logarithms, and wind share by the logit transform (10). From Fig. 2, seasonal patterns are evident in all series, as is the negative trend in emissions, E_t, and the positive in wind energy production, W_t. The very clear seasonal variation might hide the stochastic properties of the data. Therefore, the ADF tests are also implemented on detrended and de-seasonalized data, i.e., after extracting the deterministic terms 1, t, *cos*, and *sin* by regression. The series thus filtered are shown in Fig. A.1, and these are the objects that the stochastic model should describe.[12] ADF results for the filtered series are indicated as ADF* in Table 1. From the results, industrial production, *ind*, exhibits a unit root, so we will mainly use this variable in terms of growth rates (log differences) and squares, although we will include the levels in a preliminary regression, to investigate the EKC.

The other main variables do not exhibit unit roots, except that we also include the cumulated CO_2 and wind energy series in Table 1, on the grounds that it is cumulated CO_2 in the atmosphere that matters for our future. The tests fail to reject a unit root for the cumulated series. As detailed in relation to the fractional analysis in Section 5, we focus on the emissions and wind energy series without cumulation for modeling purposes.

4.1. Preliminary regression analysis

We are interested in assessing the dynamic effect of the share of wind in energy production on CO_2 emissions within a time series framework. Before proceeding to the FVECM-X$_{d,b}$ analysis, we consider a preliminary regression analysis, based on the specification

$$E_t = a + b_0 t + b_1 \sin(2\pi t/12) + b_2 \cos(2\pi t/12)$$
$$+ \sum_{i=1}^{p} b_{e,i} L^i E_t + \sum_{j=1}^{q} b_{w,j} L^j W_t + b'_x X_t + \varepsilon_t. \tag{11}$$

This allows for dynamics through the inclusion of lagged emissions and wind energy, as well as a time trend. The use of wind energy and lags as regressors to explain emissions follows Cullen (2013) and the subsequent regression literature.

Results for various specifications using climate and demand variables in X_t in (11) appear in Table 2. The baseline regression includes the trend, seasonals, $p = q = 2$ lags, and the EKC variables, to investigate the latter, as they have been studied in the literature. They get the expected signs, i.e., increasing and concave dependence of emissions on output, although the coefficients are insignificant. The negative trend in emissions and seasonality enter significantly, as they do in all specifications for emissions (baseline and specifications 1 through 3). The coefficients on wind energy are negative and significant, consistent with the idea that an increase in wind energy production reduces emissions. In the baseline specification, the LB statistic is insignificant at level 5%.

Specification 1 adds the climate variables, which are part of our main focus. Temperature gets a significantly negative coefficient, consistent with the notion that the direct demand effect dominates the indirect efficiency effect. The other climate variables are insignificant for emissions, which is a result in itself. Specification 2 replaces the EKC with the growth variables, since these are the stationary variables that will be used in the FVECM-X$_{d,b}$ analysis, so we examine what difference this switch makes in a basic regression analysis. It turns out that squared growth enters significantly, but with a positive coefficient, in contrast to the expected negative sign on the quadratic portion of the EKC. Perhaps growth volatility increases emissions more than the EKC explains anything for Denmark.

LB indicates misspecification for specifications 1 and 2, and also with more lags included, consistent with the strong persistence, so ultimately we use the fractional models to handle these residuals. From

---

[11] See http://www.cpc.ncep.noaa.gov/data/teledoc/nao.shtml.

[12] The coefficients on trend and seasonals are still estimated jointly with all other parameters in the FVECM-X$_{d,b}$.

(a) E_t

(b) W_t

(c) $temp_t$

(d) $precip_t$

(e) $sunshine_t$

(f) $NAOI_t$

(g) $\Delta \log(ind_t)$

(h) $(\Delta \log(ind_t))^2$
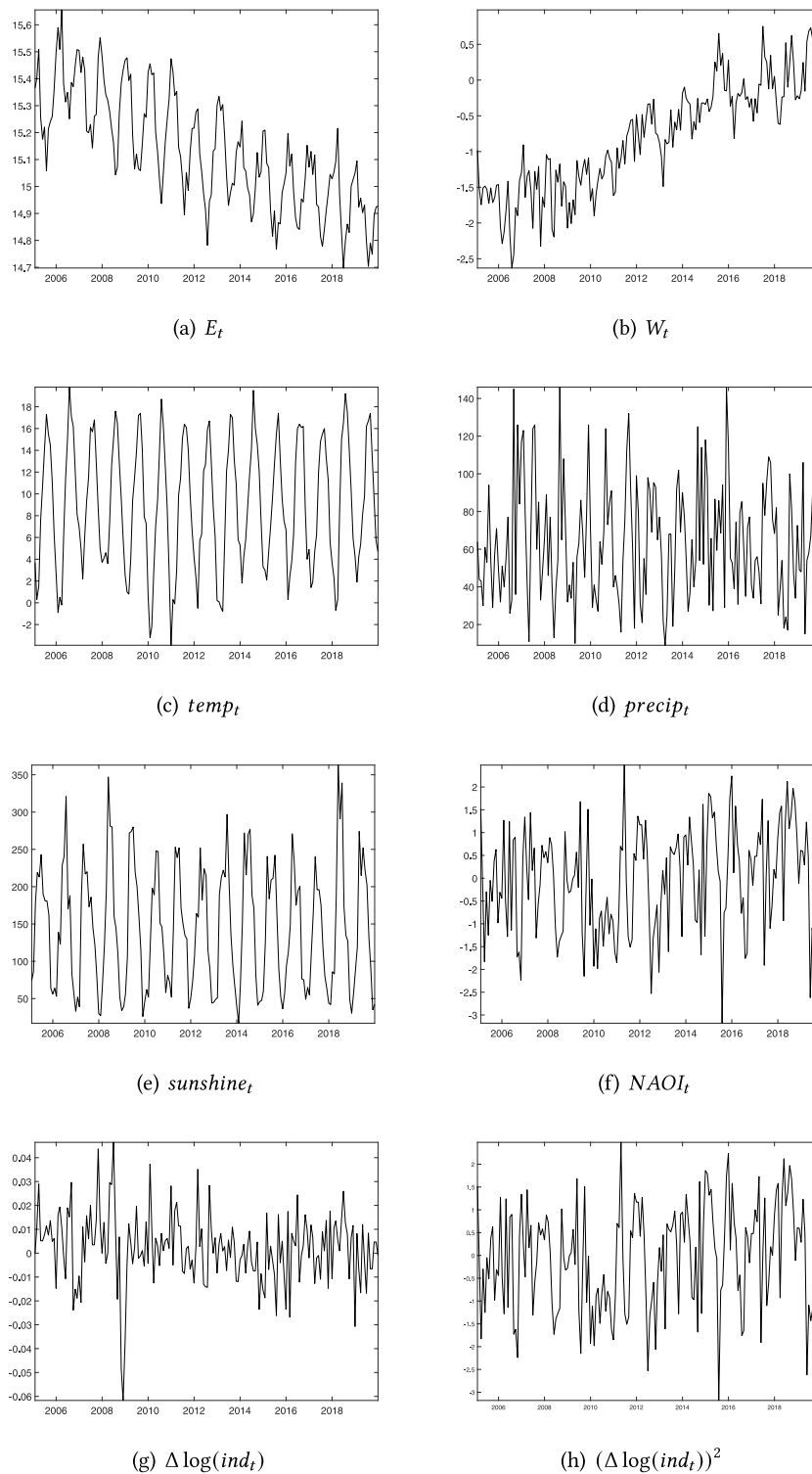
Fig. 2. Variables used for estimation of models.

(2), the residuals for the fractional models actually do not include lags (and neither do the cointegrating residuals in standard models without covariates). Therefore, specifications 3 and 4 are the regressions of E and W without lags, corresponding to (2), i.e., the dependent variable in the last column is W_t, not E_t. Wind energy production increases with precipitation, which signals stormy weather, and is negatively related to growth and its square. It is the residuals from these last two

specifications that the fractional models will handle, which is, indeed, necessary, based on the strongly significant LB statistics.[13]

---

[13] Results of a two stage procedure, directly applying the FVECM without covariates to residuals from specifications 3 and 4, are presented in Appendix B, Table B.3.

Table 2

Regression results. The table reports parameter estimates (with robust HAC standard errors in parentheses) from the regressions (11) using the monthly data series over the period January, 2005 to December, 2019. The dependent variable is wind energy $W_t = \log(w_t/(1 - w_t))$ from (10) in specification 4 (last column), and log emissions $E_t = \log(CO_{2,t})$ otherwise. The regressors include lags of E_t and W_t, a trend, seasonals, temperature, precipitation, sunshine hours, NAOI, EKC variables, and production growth and its square. The bottom lines report adjusted R^2, the Ljung–Box (LB) statistic for six periods, and the associated p-value. Superscripts a, b, and c indicate significance at level 1%, 5%, and 10%, respectively.

	Baseline	Spec1	Spec2	Spec3	Spec4
$trend$	-0.0016^a (0.0003)	-0.0015^a (0.0003)	-0.0018^a (0.0003)	-0.0029^a (0.0002)	0.0122^a (0.0008)
$\sin(2\pi t/12)$	0.0557^a (0.0088)	-0.0328^c (0.0191)	-0.0193 (0.0213)	-0.0122 (0.0248)	0.0257 (0.1086)
$\cos(2\pi t/12)$	0.1544^a (0.0077)	0.0781^a (0.0243)	0.0808^a (0.0282)	0.0704^b (0.0343)	-0.0132 (0.1460)
$temp_t$	–	-0.0994^a (0.0196)	-0.0866^a (0.0243)	-0.0860^a (0.0299)	0.0684 (0.1128)
$precip_t$	–	-0.0040 (0.0061)	-0.0032 (0.0060)	0.0089 (0.0060)	0.1178^a (0.0325)
$sunshine_t$	–	0.0187 (0.0125)	0.0108 (0.0124)	0.0061 (0.0123)	0.0229 (0.0703)
$NAOI_t$	–	-0.0023 (0.0058)	-0.0022 (0.0059)	-0.0043 (0.0066)	0.0474 (0.0289)
$\log(ind_t)$	0.1131 (0.6196)	-0.0553 (0.7119)	–	–	–
$[\log(ind_t)]^2$	-0.1210 (0.6153)	0.0399 (0.7055)	–	–	–
$\Delta\log(ind_t)$	–	–	0.0054 (0.0049)	0.0026 (0.0051)	-0.0757^b (0.0332)
$[\Delta\log(ind_t)]^2$	–	–	0.0108^a (0.0037)	0.0138^a (0.0037)	-0.0503^b (0.0238)
E_{t-1}	0.0037 (0.0023)	-0.0008 (0.0056)	-0.0005 (0.0024)	–	–
E_{t-2}	-0.0021 (0.0046)	0.0014 (0.0023)	-0.0006 (0.0039)	–	–
W_{t-1}	-0.0387^a (0.0109)	-0.0354^a (0.0101)	-0.0313^a (0.0102)	–	–
W_{t-2}	-0.0381^a (0.0111)	-0.0419^a (0.0108)	-0.0405^a (0.0115)	–	–
R^2_{adj}	0.9003	0.9185	0.9193	0.8963	0.8309
LB(6)	10.75	32.776	41.0200	114.22	59.2370
p-value	0.0964	0.0000	0.0000	0.0000	0.0000

Overall, the results from the preliminary regression analysis are consistent with the notions that measuring the impact of wind energy production on emissions is a nontrivial task, that trend, seasonality, climate, and demand variables apparently matter for the relation, but that the basic regression approach is misspecified.[14]

5. Empirical analysis

The explanation of the somewhat unsatisfactory and inconclusive regression results that we pursue is that the series are fractionally integrated, and that a fractional cointegration analysis is warranted. Table 3 reports exact local Whittle (ELW) estimates of the order d of fractional integration of the variables used in the preceding regression analysis, after removing a linear deterministic trend and seasonals, using a separate preliminary regression for each series. Results are reported for three different bandwidths, m. None of the climate or growth series appears to exhibit long memory. In contrast, the emissions and wind energy series E_t and W_t exhibit fractional integration, with $\hat{d}$ significantly positive. Thus, pre-filtering is not sufficient to purge these series for long memory, based on the two largest m values. Further, the estimates of d are significantly below unity, i.e., no unit root, consistent with the ADF results in Table 1. The results in Table 3 are consistent with a common order d for both series.

The cumulated CO_2 and wind energy series appear fractionally integrated of order greater than one, rather than unit root processes, i.e., $I(d)$, with $d > 1$, as opposed to $I(1)$, even after removal of the seasonal trend. Already the (uncumulated) emissions and wind energy series are long memory processes, $I(d)$, with $d > 0$. We have not

Table 3

Exact local Whittle (ELW) estimates of the fractional parameter d. *Filtered* indicates detrended and de-seasonalized series. The standard error of $\hat{d}$ is 0.1365 for bandwidth $m = [T^{0.5}]$, 0.1053 for $m = [T^{0.6}]$, and 0.0812 for $m = [T^{0.7}]$.

Variable	Filtered		
	$m = [T^{0.5}]$	$m = [T^{0.6}]$	$m = [T^{0.7}]$
E_t	-0.0081	0.2571	0.3775
W_t	0.1278	0.2651	0.2705
$temp_t$	0.1154	0.1731	0.3070
$precip_t$	-0.2823	0.1342	-0.0656
$sunshine_t$	-0.3971	-0.2703	-0.1733
$NAOI_t$	-0.0334	0.0042	0.1272
$\Delta\log(ind_t)$	-0.1566	-0.0683	0.0636
$\Delta\log(ind_t)^2$	0.0675	0.4571	0.0889
$cumul.$ CO_2	1.2743	1.1732	1.1373
$cumul.$ $Wind$	1.3020	1.2080	1.1426

cumulated them in the subsequent analysis. Policy decisions on wind energy adoption can impact wind energy production and emissions, so we look at these two series. Policy decisions cannot directly affect previously cumulated CO_2, only current emissions. It is cumulated CO_2 in the atmosphere that matters for our future, presumably globally cumulated CO_2. When cumulating our CO_2 series, we get cumulated Danish CO_2 emissions from energy production, not global cumulated CO_2 from all sources. The CO_2 emissions series we end up analyzing (uncumulated, Denmark, energy production) represents the portion of global cumulated CO_2 from all sources that current local wind power adoption policies can directly impact.

Fractional integration of similar order d for E_t and W_t suggests that fractional cointegration analysis can be a suitable tool for studying the relation between the two. Under correct parametric specification of

---

[14] The only insignificant LB statistic is achieved in the baseline specification, which includes a unit root regressor.

Table 4

FVECM-X$_{d,b}$ results. The table reports the results of estimation of the FVECM-X$_{d,b}$ using the monthly emissions and wind energy series E_t and W_t over the period January, 2005, through December, 2019. The Johansen and Nielsen (2012) test of fractional cointegration takes the value 11.578 (bootstrap p-value = 0.02078) for $r = 0$, and 0.7819 (bootstrap p-value = 0.3765) for $r = 1$. The estimated cointegration vector for $r = 1$ is $\hat{\beta} = (1.0000, 0.2684)$. The bootstrapped confidence interval at 90% for β_2 is (0.0969, 0.3975). The bottom panel reports Ljung–Box (LB) tests for five and ten periods, the associated p-values, and the Doornik and Hansen (2008) test of multivariate normality. The maximized value of the log-likelihood function is 250.261. MEA over 24 months is estimated to 0.1616, with bootstrap confidence interval at 90% given by (0.0446, 0.2253), and standard deviation 0.0607. MEA over 12, 36, and 48 months are 0.1616, 0.1617, and 0.1617, respectively.

	E_t				W_t			
	Est.	Std.Err.	t-stat	p-val	Est.	Std.Err.	t-stat	p-val
Estimates								
d	0.4506	0.0630	7.1512	0.0000	0.4506	0.0630	7.1512	0.0000
α	−0.3314	0.1025	−3.2346	0.0012	−0.2857	0.6327	−0.4515	0.6516
β	1.0000	–	–	–	0.2684	0.0874	3.0693	0.0021
μ	8.4260	0.0374	225.5223	0.0000	−1.6118	0.1654	−9.7438	0.0000
$trend$	−0.0026	0.0004	−6.5650	0.0000	0.0104	0.0017	6.2098	0.0000
$\sin(2\pi t/12)$	−0.0284	0.0192	−1.4795	0.1390	−0.0438	0.0933	−0.4694	0.6388
$\cos(2\pi t/12)$	0.0628	0.0237	2.6555	0.0079	−0.1198	0.1143	−1.0481	0.2946
$temp$	−0.1095	0.0199	−5.5080	0.0000	0.0170	0.0963	0.1766	0.8598
$precip$	−0.0046	0.0060	−0.7666	0.4433	0.0946	0.0284	3.3262	0.0009
$sunshine$	0.0186	0.0129	1.4394	0.1500	−0.0165	0.0612	−0.2701	0.7871
$NAOI$	−0.0069	0.0053	−1.3061	0.1915	0.0597	0.0252	2.3658	0.0180
$\Delta \log(ind)$	0.0040	0.0047	0.8365	0.4029	−0.0912	0.0224	−4.0718	0.0000
$[\Delta \log(ind)]^2$	0.0067	0.0047	1.4292	0.1529	−0.0108	0.0221	−0.4879	0.6256
Misspecification tests								
LB(5)	17.3802	–	–	0.0038	1.8981	–	–	0.8631
LB(10)	19.4823	–	–	0.0345	16.3038	–	–	0.0913
Normality	1.3133	–	–	0.8591				

long and short run components, the FVECM-X$_{d,b}$ model can deliver additional insights on the dynamics, and the impact of climate, demand, and other explanatory variables on the relation between E_t and W_t.

We estimate a bivariate version of (1)–(2), with $Y_t = (Y_{t,1}, Y_{t,2})' = (E_t - \mu_{t,1}, W_t - \mu_{t,2})'$, and the covariates X_t given by the climate and growth variables. Results appear in Table 4. BIC selects $k = 0$ lagged short-run terms, and the LR test fails to reject $k = 0$ against $k = 1$. In addition, the LR test fails to reject $d = b$ (p-value 1.000). Thus, as in classic cointegration, d and b coincide, although in the present case not at unity. This result shows that the paths of emissions and wind energy are closely tied, i.e., the error-correction term $\beta' Y_t$ with $Y_t = Z_t - \mu_t$ is a weakly dependent or $I(0)$ process, and departures from equilibrium short-lived. The same happens for other model variations in the remainder of the paper, so we present results for the restricted models, imposing $d = b$ (this follows Nielsen and Shibaev, 2018) and $k = 0$ throughout. The only exception is an FVECM model without covariates, not even trend or seasonals, i.e., $\mu_t = \mu$ in (2). In this case, BIC and the LR test point to $k = 1$, so we report results imposing this specification (Tables 5 and B.1), although this is not a very reasonable model, and really only included to illustrate the problems that arise in the case without covariates. Without covariates, $\mu_t = \mu$, the condition $d = b$ must be imposed in order for μ to be identified, because $\Delta^{d-b}\mu = 0$ for $d > b$. In principle, with time-varying covariates in (2), we should have a chance of estimating coefficients on these for $d > b$. However, in our data, the iterations toward the maximum of the log-likelihood function force b as close to d as possible. In the model in Table 4, if d and b are estimated separately, both are estimated at 0.4506, the estimated standard error of $\hat{d} - \hat{b}$ is 0.3561, and the LR test of $d = b$ gets p-value 1.000.

With $d = b$ and $k = 0$ imposed, the Johansen and Nielsen (2012) test indicates fractional cointegration with rank $r = 1$, one cointegrating relation, based on bootstrapped p-values. Thus, the estimated model reported in Table 4 is

$$\begin{bmatrix} \Delta^d Y_{t,1} \\ \Delta^d Y_{t,2} \end{bmatrix} = \begin{bmatrix} \alpha_1 \\ \alpha_2 \end{bmatrix} \begin{bmatrix} 1 & \beta_2 \end{bmatrix} \begin{bmatrix} \Delta^{d-b} L_b Y_{t,1} \\ \Delta^{d-b} L_b Y_{t,2} \end{bmatrix} + \begin{bmatrix} \varepsilon_{t,1} \\ \varepsilon_{t,2} \end{bmatrix}. \tag{12}$$

With $k = 0$, the FCVAR$_{d,b}$ and FVECM$_{d,b}$ coincide, implying that the asymptotic inference theory for the former applies (of course, we include covariates, as well, in the FVECM-X$_{d,b}$). The estimate of d is .45 and significantly different from both 0 and 1 at conventional levels.

This indicates that E_t and W_t taken in deviation from the climate and growth variables exhibit long memory around the linear and seasonal trend, as $d < .5$, i.e., in the stationary range. Thus, climate and demand matter. The effect of a shock persists for a long period of time, reflecting long memory (fractional integration), and the series follow paths that are tied together in the long run, as indicated by the cointegration rank. On the other hand, there is no unit root, which would be the case if $d = 1$, so the long run equilibrium is more appropriately studied in the FVECM than in the classic cointegrated VECM. Further, the LB and Doornik and Hansen (2008) tests (bottom panel) show no (or only mild) signs of misspecification.

The parameter β_2 is estimated to 0.2684, indicating a negative relation between CO_2 emissions and wind energy production in the model in Table 4. When W_t increases, E_t must decrease in order to maintain the stable equilibrium relation, i.e., to bring the error correction term or cointegration residual given by $\beta' Y_t = E_t - \mu_{1,t} + \beta_2(W_t - \mu_{2,t})$ back toward zero, or E_t toward $\mu_{1,t} - \beta_2(W_t - \mu_{2,t})$, with $\beta_2 > 0$. The parameters governing the adjustment to this equilibrium, α, are both negative, although only the coefficient for emissions is significant. From the signs, if either variable is too large, relative to the levels given by the deterministic trend, seasonal, climate, and growth variables, both will subsequently be reduced, with E_t moving faster toward the equilibrium than W_t.

Predicted values of each coordinate of μ_t from (2) are plotted against time in Exhibits (a) and (b) of Fig. 3, along with the original series E_t and W_t. Evidently, $\hat{\mu}_t$ provides a good fit to the emissions and wind energy series, hence indicating the relevance of the explanatory variables. From the results in Table 4, the deterministic trend component of μ_t is strongly significant for both E_t and W_t, as is one of the seasonal terms for E_t. The results further confirm that higher temperature reduces emissions, i.e., the direct demand effect dominates the indirect efficiency effect, and that precipitation and North Atlantic oscillations increase wind power production, consistent with the notion that they signal stormy weather, hence facilitating wind power production. The dominant effect of the demand variables turns out to be a negative relation between wind energy and industrial production growth. Exhibits (c) and (d) of Fig. 3 display the ACFs of the fitted FVECM-X$_{d,b}$ residuals ($\hat{\varepsilon}_{t,1}$, $\hat{\varepsilon}_{t,2}$) from (12). Almost all autocorrelation present in the original data is explained by the estimated model, leaving nearly uncorrelated residual series.
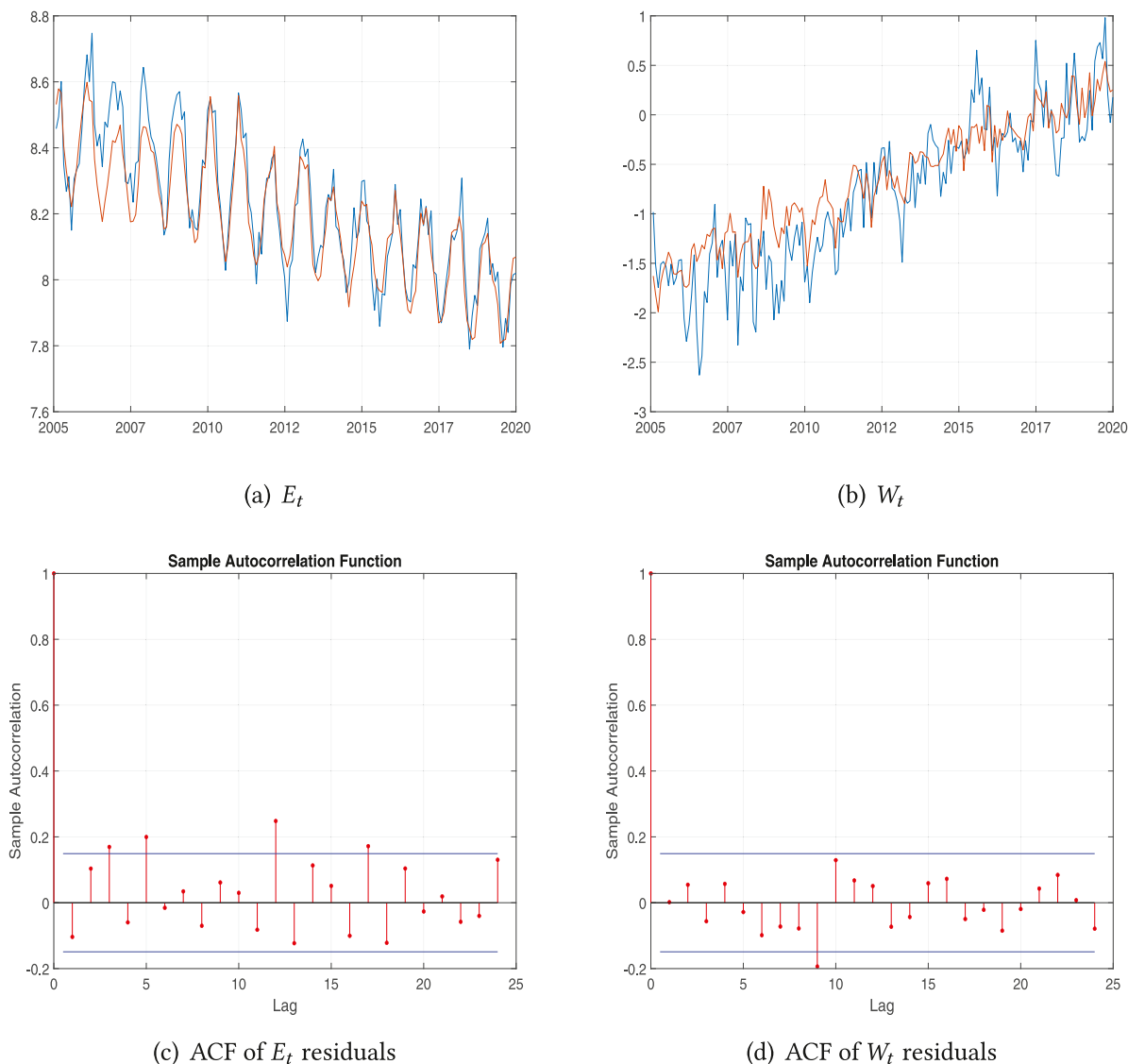
(a) E_t

(b) W_t

(c) ACF of E_t residuals

(d) ACF of W_t residuals

Fig. 3. Predicted μ_t components and residual ACFs. Exhibits (a) and (b) show the E_t and W_t series (blue lines) and the predicted values of the associated components of μ_t from (2) (red lines) from the estimated FVECM-X$_{d,b}$ model (12). Exhibits (c) and (d) show the autocorrelation functions (ACFs) for the fitted residual series $\hat{\varepsilon}_{t,1}$, $\hat{\varepsilon}_{t,2}$ from the estimated model, with 95% confidence bands shown in blue.

Fig. 4 shows the two series, adjusted for covariates, and their cointegrating relation. Exhibit (a) shows $E_t - \hat{\mu}_{1,t}$ (blue line) and $-\beta_2(W_t - \hat{\mu}_{2,t})$ (red line). Exhibit (b) illustrates the cointegrating relation between emissions and wind energy production, corrected for covariates. The series are moving together in the long run, and the error correction term does not exhibit the similar long run movements as the two series, so we interpret the relation as not spurious.

To get a more complete understanding of the dynamic relation, we compute the impulse response function (IRF) from wind energy to emissions, and viceversa, based on the estimated FVECM-X$_{d,b}$ model, and shown in Fig. 5, along with bootstrapped 90% confidence bands. The IRF in the left exhibit, $\mathrm{IRF}_{W \to E}(i)$, shows the response after i months, i.e., of E_{t+i}, $i = 0, \dots, 25$, to a W_t impulse, namely, a shock to $\varepsilon_{t,2}$ from (12) of size one standard deviation, $\sigma_W = \sigma(\varepsilon_{t,2})$, so $\mathrm{IRF}_{W \to E}(i) = \sigma_W \frac{\partial E_{t+i}}{\partial \varepsilon_{t,2}}$, with $\mathrm{IRF}_{E \to W}(i)$ defined analogously (in the right exhibit). From the figure, a positive impulse from either variable induces a negative response in the other, thus reinforcing that a system analysis, such as the FVECM-X$_{d,b}$, is called for. The causal effect of wind energy on emissions cannot be identified in a regression or engineering approach.

The response in the left exhibit in Fig. 5, the reduction in E_t following an increase in W_t, is the main effect of our concern. The significant result confirms the potential of wind energy for CO_2 abatement. The negative response in the right exhibit may indicate that observed reductions in emissions are viewed as signs of success and encourage further investments in green technology. This ties in with the possibility of endogeneity of the policy response. Below, we fail to reject that wind energy is weakly exogenous, but the IRF clearly reveals a reaction, so the variable does not appear strongly exogenous. The emissions reduction following an increase in wind energy remains significant for more than six months, whereas the wind power production response to an emissions impulse only remains significant for two months.

To quantify the impact of wind power production on emissions, we use $\mathrm{IRF}_{W \to E}(i)$ for $\partial E / \partial W$, and estimate the proportional impact of wind penetration w from (5) as $\partial E / \partial w = \mathrm{IRF}_{W \to E}(i) / [w(1-w)]$. Wind penetration w averages 32.8% over the period, cf. Table 1, with $\partial W / \partial w = 1 / [w(1-w)]$ averaging 5.561. Combining with the estimated IRF, a one percentage point increase in the share of wind in total energy production is predicted to generate a reduction in CO_2 emissions of the order 0.01% within the first month, and a long-run cumulated reduction over 24 months of the order 0.11%. To assess the MEA arising
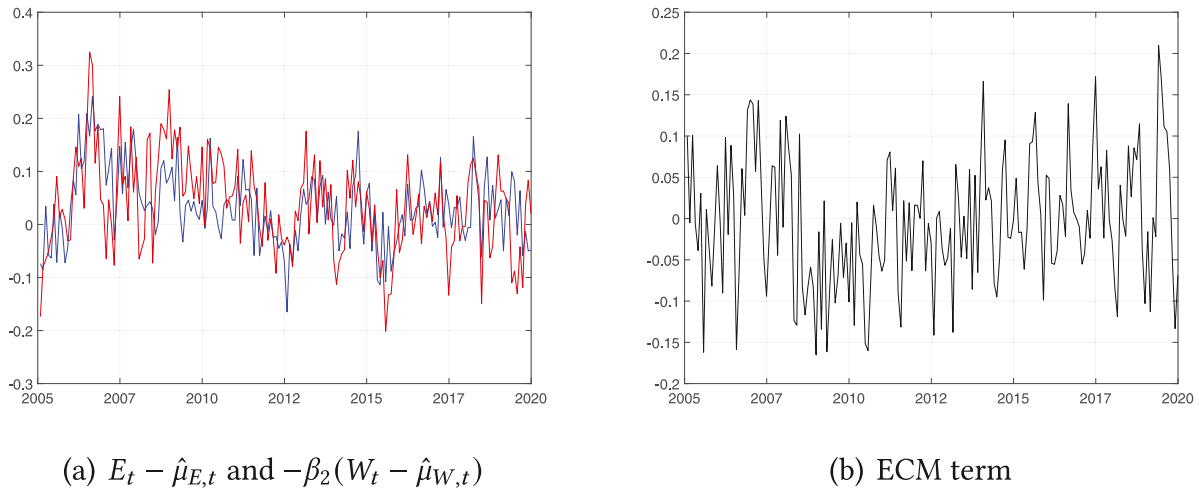
(a) $E_t - \hat{\mu}_{E,t}$ and $-\beta_2(W_t - \hat{\mu}_{W,t})$

(b) ECM term

Fig. 4. Comovement. Exhibit (a) illustrates $E_t - \hat{\mu}_{1,t}$ (blue line) and $-\beta_2(W_t - \hat{\mu}_{2,t})$ (red line). Exhibit (b) illustrates the cointegrating relation between emissions and wind energy production, corrected for covariates.
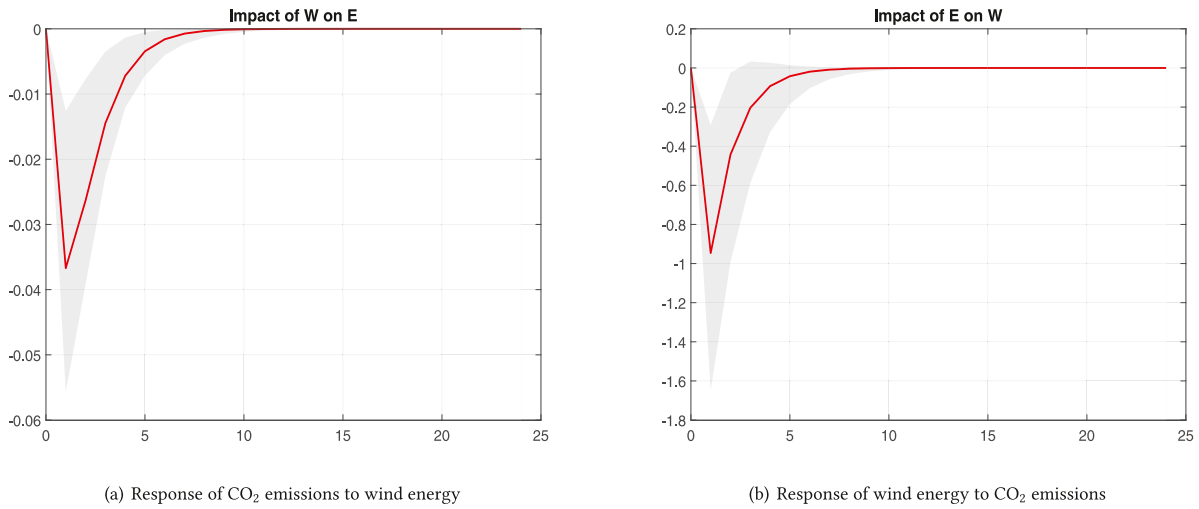

(a) Response of CO_2 emissions to wind energy

(b) Response of wind energy to CO_2 emissions

Fig. 5. Impulse-response functions from FVECM-X$_{d,b}$. In gray the bootstrapped 90% confidence bands. MEA over 24 months is estimated to 0.16. The residual standard deviations are $\sigma_E = 0.0572$ and $\sigma_W = 0.2796$.

from the increasing wind power production, the latter result is adjusted for emission intensity EI = $CO_2/Prod$ (see (5) and (9)), i.e.,

$$\text{MEA} = -\sum_{i=1}^{24} \text{IRF}_{W \to E}(i) \frac{\text{EI}}{w(1-w)} . \tag{13}$$

Essentially, the adjustment takes the impact from the level of E_t, W_t to the raw data, $CO_{2,t}$, $Wind_t$.[15] With EI = 1.399 tCO_2/MWh over the period, MEA is estimated at 0.16, in tonnes of CO_2 emissions avoided per additional MWh of wind energy produced. Although system dependent, MEA estimates in the regression literature tend to range between 0.3 and 0.7, with some concentration between 0.4 and 0.6, broadly consistent with the original estimate by Cullen (2013), at 0.43. Clearly, our estimate is low, relative to those in the literature. This could indicate that additional abatement in Denmark is hard, with wind penetration already relatively high, but is also consistent with the

possibility of regressions being misspecified, and endogeneity having a mitigating effect on the abatement potential.[16]

5.1. Sensitivity to model specification

Several model variations are summarized in Table 5. If the explanatory variables, i.e., the trend, seasonal, climate, and growth variables, are dropped, then the FVECM-X$_{d,b}$ from (1)–(2) reduces to a standard FVECM. This is the special case imposing the restriction $\mu_t = \mu$ in (2), controlling only for initial values. Several coefficients on the explanatory variables are significant in Table 4, thus indicating the relevance of the extended model. Results from estimation of the restricted FVECM appear in Appendix B, Table B.1. The maximized value of the log-likelihood function drops by more than 120, relative to the FVECM-X$_{d,b}$ in Table 4, and the LR test rejects the FVECM at all conventional levels. MEA drops to 0.07 and is insignificant. The results reinforce the relevance of accounting for explanatory variables in the FVECM-X$_{d,b}$, and suggest that the potential of wind energy for CO_2 abatement may understated in the misspecified model.

---

[15] While EI $\partial W/\partial w = 7.780$, the sample average of $CO_{2,t}/[Prod_t w_t(1-w_t)]$ is 7.791. The persistence in series implies that it makes little difference whether averaging is before or after using the derivative formula.

[16] Beside the regression literature, CDS report high MEA, too, at 0.69, using seasonally pre-adjusted data over the shorter period ending in 2017 and total IRF (i.e., not around the seasonal trend) from a model without covariates.

Table 5

Summary table. For each FVECM-X$_{d,b}$ model, the table reports estimated d, with estimated standard error in parenthesis, estimated β_2 and MEA, with 90% bootstrap confidence intervals in square brackets, maximized value of the log-likelihood function, and p-value of the LR test of $k = 0$ against $k = 1$.

Feature	Table	d	β_2	MEA	Loglik	$k = 0$
Baseline	4	0.4506 (0.0630)	0.2684 [0.0969,0.3975]	0.1616 [0.0446,0.2253]	250.261	0.0988
Only deterministic	6	0.4245 (0.0703)	0.2238 [0.1324,0.2913]	0.1601 [0.0699,0.2583]	205.741	0.1817
Fuel and electricity prices	8	0.4986 (0.0660)	0.2406 [0.1054,0.2980]	0.2040 [0.0944,0.3772]	256.091	0.1649
Only level	B.1	0.8136 (0.1219)	0.2581 [0.1923,0.3199]	0.0713 [−0.6877,1.0412]	121.762	0.0015
Raw data	B.2	0.4985 (0.0621)	4.2790 [−1.8629,6.7881]	0.0852 [−0.0379,0.1799]	280.942	0.0728
Two stage	B.3	0.4120 (0.0632)	0.2866 [0.1885,0.4091]	0.1387 [0.0229,0.2174]	245.563	0.1271
W_t weakly exogenous	B.4	0.4377 (0.0540)	0.2667 [0.1474,0.4690]	0.1645 [0.0571,0.2347]	250.160	0.1141
No waste	B.5	0.4526 (0.0628)	0.2746 [0.1313,0.3696]	0.1736 [0.0781,0.2741]	249.644	0.0969
Biomass	B.6	0.4489 (0.0617)	0.2763 [0.0428,0.3730]	0.1222 [0.0103,0.2212]	263.609	0.0850
Trivar. fuel	B.8	0.5883 (0.0629)	0.2456 [0.0684,0.3410]	0.1928 [0.0818,0.3142]	497.424	0.0561
Trivar. electricity	B.9	0.5849 (0.0616)	0.2351 [0.0348,0.4007]	0.1112 [0.0330,0.2900]	428.251	0.0591

Table 6

FVECM-X$_{d,b}$ results with deterministic terms. The table reports the results of estimation of the FVECM-X$_{d,b}$ with deterministic terms using the monthly emissions and wind energy series E_t and W_t over the period January, 2005, through December, 2019. The Johansen and Nielsen (2012) rank test indicates fractional cointegration with $r = 1$ (LR = 12.9504 (bootstrap p-value = 0.0115) for $r = 0$, LR = 1.1909 (bootstrap p-value = 0.2751) for $r = 1$). The estimated cointegration vector for $r = 1$ is $\hat{\beta} = (1.0000, 0.2238)$. The bottom lines report Ljung–Box (LB) tests for five and ten periods, the associated p-values, and the Doornik and Hansen (2008) test of multivariate normality. The maximized value of the log-likelihood function is 205.741. MEA is estimated to 0.1601, with bootstrap confidence interval at 90% given by (0.0699,0.2583), and standard deviation 0.0587.

	E_t				W_t			
	Est.	Std.Err.	t-stat	p-val	Est.	Std.Err.	t-stat	p-val
Estimates								
d	0.4245	0.0703	6.0352	0.0000	0.4245	0.0703	6.0352	0.0000
α	−0.4608	0.1469	−3.1377	0.0017	−0.7659	0.7785	−0.9838	0.3252
β	1.0000	–	–	–	0.2238	0.0527	4.2502	0.0000
μ	8.4354	0.0409	206.2506	0.0000	−1.6537	0.1916	−8.6310	0.0000
trend	−0.0026	0.0004	−6.9031	0.0000	0.0108	0.0018	6.0889	0.0000
$\sin(2\pi t/12)$	0.0681	0.0091	7.5190	0.0000	−0.1168	0.0432	−2.7024	0.0069
$\cos(2\pi t/12)$	0.1483	0.0090	16.4997	0.0000	−0.0634	0.0428	−1.4793	0.1391
Misspecification tests								
LB(5)	3.7595	–	–	0.5845	6.9761	–	–	0.2224
LB(10)	5.9018	–	–	0.8234	12.6608	–	–	0.2433
Normality	4.4342	–	–	0.3504				

Estimation of the FVECM-X$_{d,b}$ on the raw CO_2 and wind energy production data, $Z_t = (CO_{2,t}, Wind_t)'$, rather than $Z_t = (E_t, W_t)'$ used so far, cf. (9)–(10), yields the results in Appendix B, Table B.2. In this case, the Doornik and Hansen (2008) test of multivariate normality rejects at the 1% level, in stark contrast to the p-value of 0.86 in Table 4. With raw data (Table B.2), the IRFs in Fig. B.2 are insignificant throughout, leading to a MEA estimate that is low, at 0.09, and insignificant, as well. From the results, the log of emissions and logit of wind share transformations (9)–(10) render the series amenable to analysis based on Gaussianity, whereas the present model is misspecified for the raw data, hence leading to implausible conclusions.

Table B.3 shows results from a two stage procedure that should be asymptotically close to equivalent to the one stage procedure otherwise used. Residuals from specifications 3 and 4 in Table 2 are analyzed using the standard FVECM without covariates. Thus, the first stage is the estimation of (2) by ordinary regression, without lags. The dynamics of the resulting residuals are handled by the fractional model. The effect of estimated as opposed to correct residuals vanishes asymptotically as seen by repeated use of Cauchy–Schwarz (we are not giving the asymptotic derivations). We find that the one stage and two stage procedures yield very similar results for α, β, d, and MEA. This lends support to the notion that the two are asymptotically nearly equivalent and, therefore, that the one stage procedure is asymptotically well-behaved, since the two stage procedure should be so, with the asymptotic theory for the FVECM without covariates and $k = 0$ already established.

5.2. Weak exogeneity

The negative response of wind energy to emissions in Fig. 5, exhibit (b), may reflect an endogenous policy response, i.e., observed reductions in emissions encourage further investments in wind power production. Thus, it is relevant to the test the weak exogeneity of W_t with respect to E_t. To simplify exposition, consider the FVECM-X$_{d,b}$ for $k = 1$, $c = 1$, i.e.,

$$\Delta^d Y_t = \alpha\beta'\Delta^{d-b}L_b Y_t + \Gamma\Delta^d Y_{t-1} + \varepsilon_t, \quad (14)$$

where

$$Y_t = \begin{bmatrix} Y_{t,1} \\ Y_{t,2} \end{bmatrix}, \quad \alpha = \begin{bmatrix} \alpha_1 \\ \alpha_2 \end{bmatrix}, \quad \Gamma = \begin{bmatrix} \Gamma_1 \\ \Gamma_2 \end{bmatrix}, \quad \varepsilon_t = \begin{bmatrix} \varepsilon_{t,1} \\ \varepsilon_{t,2} \end{bmatrix},$$

$$V(\varepsilon_t) = \begin{bmatrix} \Omega_{11} & \Omega_{12} \\ \Omega_{21} & \Omega_{22} \end{bmatrix}.$$

Eq. (14) can be decomposed into a conditional model of $Y_{t,1}$ given $Y_{t,2}$,

$$\Delta^d Y_{t,1} = \omega\Delta^d Y_{t,2} + (\alpha_1 - \omega\alpha_2)\beta'\Delta^{d-b}L_b Y_t + (\Gamma_1 - \omega\Gamma_2)\Delta^d Y_{t-1} + \varepsilon_{t,1} - \omega\varepsilon_{t,2}, \quad (15)$$

obtained by adding the first equation of the system in (14) and the second equation multiplied by $-\omega = -\Omega_{12}\Omega_{22}^{-1}$, and a marginal model for $Y_{t,2}$, given by

$$\Delta^d Y_{t,2} = \alpha_2\beta'\Delta^{d-b}L_b Y_t + \Gamma_2\Delta^d Y_{t-1} + \varepsilon_{t,2}.$$

The conditional model in (15) contains the same information as the full model (14) when $Y_{t,2}$ is weakly exogenous. It can be shown that $Y_{t,2}$ is weakly exogenous if $\alpha_2 = 0$. In this case, the conditional model is given by

$$\Delta^d Y_{t,1} = \omega \Delta^d Y_{t,2} + \alpha_1 \beta' \Delta^{d-b} L_b Y_t + (\Gamma_1 - \omega \Gamma_2) \Delta^d Y_{t-1} + \varepsilon_{t,1} - \omega \varepsilon_{t,2}.$$

Weak exogeneity implies that $\Delta^d Y_{t,2}$ does not react to disequilibrium errors, but to lags of Y_t. Johansen (1992) considered the case $d = b = 1$, i.e., weak exogeneity in the CVAR.

Thus, verifying the weak exogeneity of W_t entails a test on the speed of convergence coefficient α_2, where the null hypothesis $\mathcal{H}_0 : \alpha_2 = 0$ is compared against the alternative $\mathcal{H}_0 : \alpha_2 \neq 0$. From Table 4, we obtain a t-statistic of -0.4515, meaning that we fail to reject the null $\mathcal{H}_0$. Hence, the statistical evidence suggests that in the FVECM-X$_{d,b}$, the variable W_t can be considered weakly exogenous with respect to E_t, given that the dependence on trend, seasonal, climate, and growth variables is taken into account.

Results for the restricted FVECM-X$_{d,b}$ imposing $\alpha_2 = 0$ appear in Appendix B.4, Table B.4. Estimates and significance of all other parameters are similar to those for the unrestricted model in Table 4. The difference in log-likelihood values confirms the result from the t-test, that W_t is weakly exogenous. IRFs with this restriction imposed are shown in Fig. B.4, Appendix B.4. While the restricted emissions response to changes in wind energy (left exhibit) mirrors the unrestricted in Fig. 5, the wind energy response to emissions, right exhibit, now remains significant for six months, too, as opposed to only two in Fig. 5. Thus, accounting for the weak exogeneity of wind energy leaves the IRF from emissions to wind energy as long-lived as the reverse IRF. Correspondingly, MEA is estimated slightly higher than in the unrestricted model. The results are consistent with the notion that policy makers exercise discretion, and that treating wind energy production decisions as exogenous shifts captures this better than leaving them endogenous, corresponding to a feedback rule. Thus, the policy tool appears more powerful, based on the restricted estimation. Still, as the resulting increase in MEA is only marginal, the main conclusion from the exogeneity analysis is that the unrestricted FVECM-X$_{d,b}$ delivers reliable inference.

5.3. Sensitivity to emissions measure

Combustion of waste constitutes a considerable portion of conventional power production in Denmark, alongside combustion of fossil fuels, and we include emissions from waste burning in our measure of CO_2. Since this represents an innovation, relative to CDS, we compare results with and without emissions from waste burning included. Results with waste burning excluded, i.e., using $CO_{2,t}$ with $S = 3$ from (4) in E_t from (9), are in Appendix B.5, Table B.5. Based on these, MEA is estimated at 0.17. Parameter estimates and significance are similar to those in Table 4, in which waste burning is included, with MEA estimated at 0.16. The slightly lower emissions abatement potential of wind energy indicated when including waste burning is consistent with the latter being the cleaner, but frequently the marginal generation method.

Biomass fuels are combusted for energy generation, too. They are usually included in a country's energy and CO_2 emissions accounts for information, only, as consumption is assumed to equal regrowth. However, it is debatable whether to consider biomass a renewable source. It can be argued to be CO_2-neutral in the long run, but this requires replanting of vegetation to absorb CO_2 in the future. Denmark is importing biomass for combustion, e.g., wood pellets from Eastern Europe, and has been criticized for burning biomass from countries where forest replanting is not always regulated. If trees are not replanted abroad, importing biomass contributes to the problem of carbon leakage, i.e., that reductions in emissions in one country can lead to increases in another.

As a first gauge of the importance of this issue for the abatement potential of wind energy, we construct an expanded emissions measure, with emissions from the burning of biomass included, i.e., using $CO_{2,t}$ with $S = 5$ from (4) in E_t from (9). Data on consumption, $C_{5,t}$, are obtained from DEA. For the emissions factor, $IEF_{5,t}$, since emissions from biomass are not part of the official statistics, we estimate a figure based on values indicated by IPCC in their GHG guidelines.[17] IPCC indicates 29.9 kg/GJ for solid biomass, and 30.6 kg/GJ for gas biomass. As our consumption measure from DEA actually includes solid biomass, biogas, and solar, with most of the weight on solid biomass (wood pellets), we use $IEF_{5,t} = 30.0$.

Results with emissions from the burning of biomass included are in Table B.6. Again, they are similar to those without biomass in Table 4. From the IRF based on the results including biomass, MEA is estimated at 0.12. This reinforces that including a relatively clean, but frequently marginal generation method in the emissions measure reduces the estimated abatement potential of wind energy.

Of course, if carbon leakage exists, it should be addressed by including all relevant emissions in the official statistics. Based on our findings, this will not necessarily make the abatement potential of wind energy look stronger, but this is a measurement problem. The true potential is best identified by including all relevant sources in the emissions measure. Indeed, if the carbon leakage problem is severe, the IPCC figures might be understated. In this case, the burning of biomass will count as less clean if carbon leakage is fully accounted for, and this can be expected to bring estimated MEA back up toward the value of 0.16 based on the results in Table 4. The latter still appear relatively robust, judging from the results of varying the emissions variable.

5.4. Long-term forecasting

Results from estimation of the FVECM-X$_{d,b}$ including only the deterministic terms (trend and seasonals) in μ_t are given in Table 6. Exclusion of X_t corresponds to the restriction $\Lambda = 0$ on (2). Comparing the results in Tables 4 and 6, log-likelihood decreases by more than 40, and the LR test rejects the restriction, i.e., climate and growth variables matter. On the other hand, the LB and normality tests in Table 6 show no sign of misspecification whatsoever, and the possibility to include deterministic variables in FVECM-X$_{d,b}$ provides a potentially powerful tool, so we explore this model a bit further.

Three of the four seasonality terms are significant at conventional levels in the model with deterministic terms, compared to only one in the model with further covariates. In both models, the speed of adjustment coefficients α are negative, with only that for emissions significant, but estimates are larger in magnitude in the model with deterministic terms, and the IRFs, shown in Fig. 6, more significant than those in Fig. 5. The resulting MEA is 0.16 with deterministic terms, confirming the value with climate and growth variables included.

Long-term forecasts and associated confidence bands are shown in Fig. 7. Transforming back to CO_2 and wind share in energy production w_t using the exponential and logistic (inverse logit), cf. (9)–(10), the 95% confidence intervals for CO_2 emissions by 2030 and 2050 are $[1963.9, 2772.2]$ and $[1071.2, 1526.0]$, respectively, in thousands of tonnes, and those for the wind share $[0.726, 0.946]$ and $[0.970, 0.996]$.

The Danish government has announced goals of 70% reduction in greenhouse gas (GHG) emissions by 2030, relative to the UN base year of 1990 levels, and 100% no-fossil energy production (corresponding to $w_t = 1$) by 2050, in accordance with the 2015 Paris Agreement joined by most countries of the world. By 2019, the reduction in CO_2 emissions relative to 1990 was already 34%. However, the 2030 confidence interval corresponds to reductions between 37% and 56%, indicating that the country is not yet on track to meet the 2030 goal with respect

---

[17] Revised 1996 IPCC Guidelines for National Greenhouse Inventories: Workbook, Module 1, Energy.
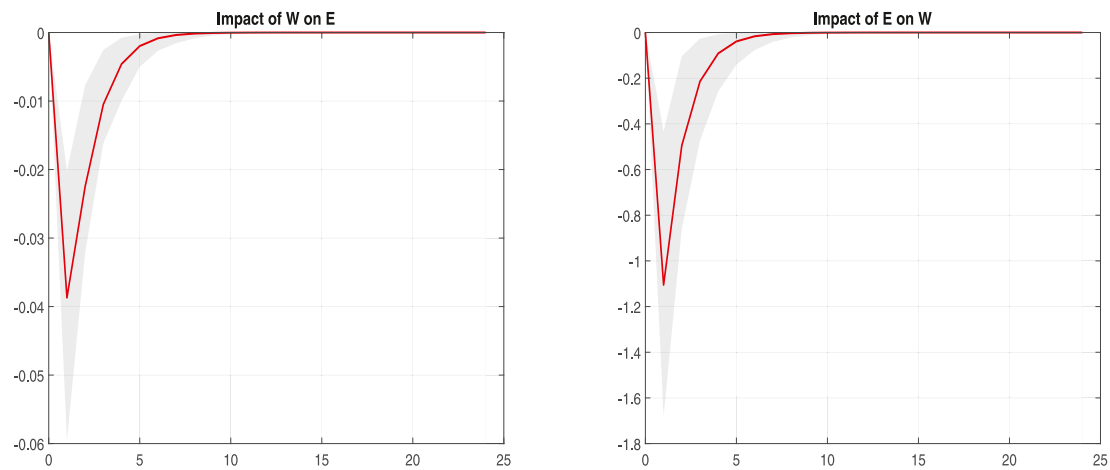
(a) Response of CO_2 emissions to wind energy

(b) Response of wind energy to CO_2 emissions

Fig. 6. Impulse-response functions from FVECM-$X_{d,b}$ with deterministic terms. In gray the bootstrapped 90% confidence bands. MEA over 24 months is estimated to 0.16.
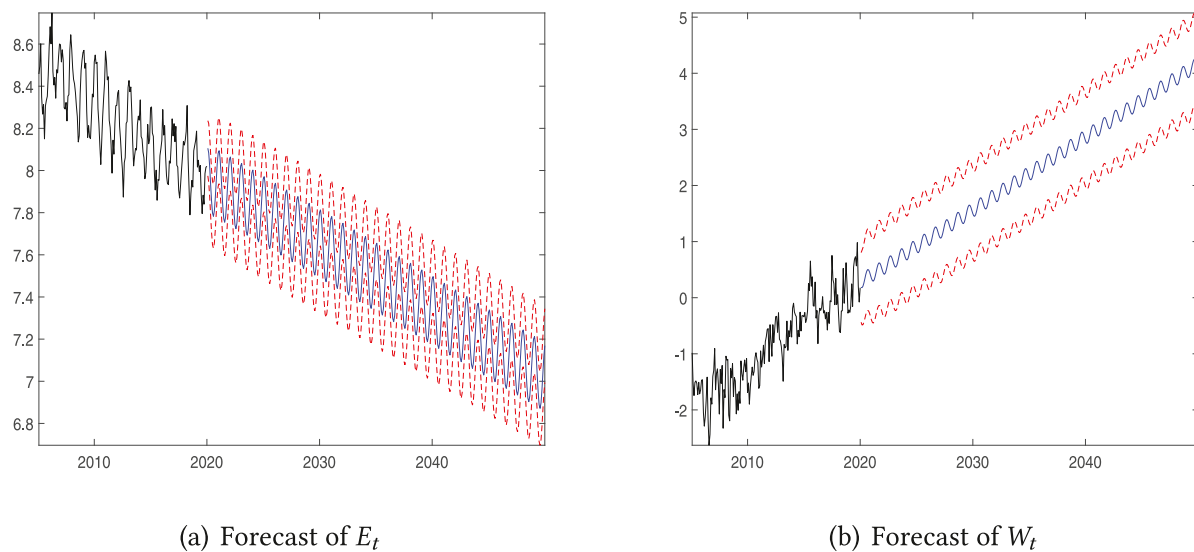
(a) Forecast of E_t

(b) Forecast of W_t

Fig. 7. Long-term forecasts of E_t and W_t based on FVECM-$X_{d,b}$ with deterministic terms. In red the 95% confidence band. In black the observed series.

5.5. Fuel and electricity prices

to CO_2 emissions (there are other GHGs). For wind share, the 2050 confidence band nearly reaches unity, which would achieve the policy goal by wind alone, and there are other no-fossil sources, such as solar and, depending on definitions, waste burning, and biomass.[18]

For comparison, we also estimate a VAR(2) model with the same deterministic terms (trend and seasonals). Results from estimation of the VAR(2) model are given in Appendix B.6, Table B.7, IRFs are shown in Fig. B.7, and long-term forecasts in Fig. B.8. The VAR(2) IRFs are poorly estimated and insignificant. The upshot is a lower MEA, at 0.08. As the long memory properties are significant in the FVECM-$X_{d,b}$, the results support the notion that ignoring fractional integration, when present, can lead to understatement of the emissions abatement potential of wind energy.

An increase in wind power production can potentially cause a drop in fuel prices, hence mitigating the impact on emissions of the increase in wind power. Similarly, an increase in the supply of wind power production can potentially reduce power prices, which can partially offset the reduction in conventional production stemming from the increase in wind energy. Thus, the general equilibrium impact of wind power production on emissions potentially falls short of estimates that ignore the supply and demand effects operating via input (fuel) or output (power) prices. To investigate this possibility, we include prices in the analysis. Although electricity prices have been considered in the regression literature, e.g., Amor et al. (2014), Di Cosmo and Valeri (2018b), and Abrell et al. (2019), fuel prices have not been considered. Here, we include the world fuel price index (WFPI), obtained from IndexMundi, as $fuel = \log(\text{WFPI})$, and EL, the electricity spot price index in Denmark, obtained from Nord Pool, as $el = \log(\text{EL})$, among the covariates in the FVECM-$X_{d,b}$.

---

[18] In fact, for wind share near unity, emissions should be zero, cf. (8), a restriction not imposed on the fractional model.

Table 7

Summary statistics for fuel and electricity prices. The table reports summary statistics for the monthly data series over the period January, 2005 through December, 2019. *Raw* refers to estimates of the fractional parameter d obtained by ELW estimation on the original series, while *Filt* indicates estimation on the detrended and de-seasonalized series. The standard errors of $\hat{d}$ are 0.1053 with $m = [T^{0.6}]$ and 0.0812 with $m = [T^{0.7}]$.

| Variable	Monthly				$\hat{d}$				Ljung–Box	
	Mean	Std.Dev.	ADF	p-val	Raw (0.6)	Raw (0.7)	Filt (0.6)	Filt (0.7)	stat	p-value
$fuel_t$	4.5028	0.2979	−2.8116	0.1953	0.9159	1.1559	0.9691	1.1393	737.84	0.0000
el_t	38.959	10.988	−3.5203	0.0405	0.7843	0.8185	0.8517	0.7595	429.24	0.0000

Table 8

FVECM-X$_{d,b}$ with fuel and electricity prices. The table reports the results of estimation of the FVECM-X$_{d,b}$ with fuel and electricity prices using the monthly emissions and wind energy series E_t and W_t over the period January, 2005, through December, 2019. The Johansen and Nielsen (2012) rank test indicates fractional cointegration with $r = 1$ (LR = 14.184 (bootstrap p-value = 0.0067) for $r = 0$, LR = 0.7534 (bootstrap p-value = 0.3853) for $r = 1$. The estimated cointegration vector for $r = 1$ is $\hat{\beta} = (1.0000, 0.2406)$. The bottom lines report Ljung–Box (LB) tests for five and ten periods, the associated p-values, and the Doornik and Hansen (2008) test of multivariate normality. The value of the log-likelihood function is 256.091. MEA is estimated to 0.2040, with bootstrap confidence interval at 90% given by (0.0944, 0.3772).

|	E_t				W_t			
	Est.	Std.Err.	t-stat	p-val	Est.	Std.Err.	t-stat	p-val
Estimates								
d	0.4986	0.0660	7.5572	0.0000	0.4986	0.0660	7.5572	0.0000
α	−0.3825	0.0997	−3.8354	0.0001	−0.2502	0.6088	−0.4110	0.6811
β	1.0000	–	–	–	0.2406	0.0527	4.5639	0.0000
μ	8.4107	0.0398	211.2191	0.0000	−1.5212	0.1828	−8.3237	0.0000
$trend$	−0.0025	0.0004	−5.6746	0.0000	0.0100	0.0020	5.0305	0.0000
$\sin(2\pi t/12)$	−0.0150	0.0199	−0.7558	0.4498	−0.1322	0.0955	−1.3846	0.1662
$\cos(2\pi t/12)$	0.0718	0.0237	3.0250	0.0025	−0.1854	0.1131	−1.6386	0.1013
$temp$	−0.1003	0.0201	−4.9965	0.0000	−0.0514	0.0960	−0.5353	0.5925
$precip$	−0.0033	0.0059	−0.5559	0.5783	0.0872	0.0274	3.1803	0.0015
$sunshine$	0.0192	0.0126	1.5195	0.1286	−0.0155	0.0588	−0.2637	0.7920
$NAOI$	−0.0053	0.0052	−1.0202	0.3076	0.0555	0.0246	3.5515	0.0238
$\Delta\log(ind)$	−0.0040	0.0074	−0.5380	0.5906	−0.0301	0.0344	−0.4507	0.3811
$[\Delta\log(ind)]^2$	0.0040	0.0047	0.8477	0.3966	0.0024	0.0218	0.1115	0.9112
Δel	0.0126	0.0063	2.0127	0.0441	−0.0780	0.0288	−2.7057	0.0068
$\Delta fuel$	−0.0049	0.0053	−0.9110	0.3623	−0.0001	0.0250	−0.0034	0.9973
Misspecification tests								
LB(5)	14.5412	–	–	0.0125	1.2219	–	–	0.9428
LB(10)	18.7034	–	–	0.0442	14.9629	–	–	0.1334
Normality	3.6542	–	–	0.4548				
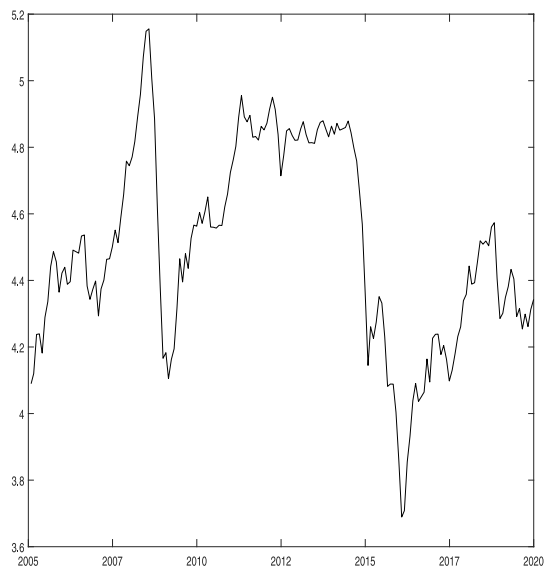
(a) *fuel*
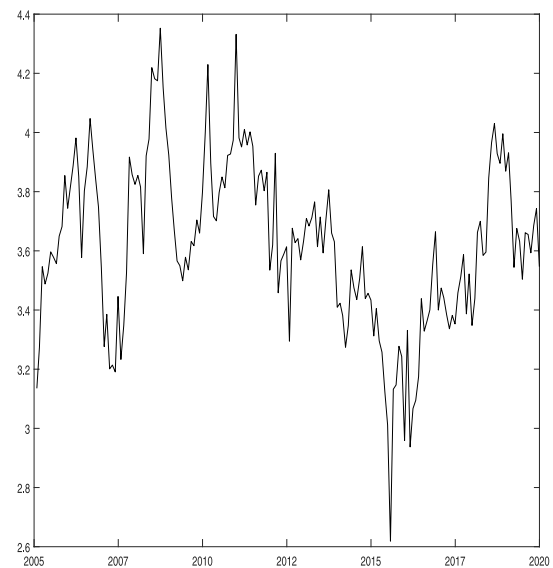
(b) *el*

Fig. 8. Price variables: World fuel price index *fuel* and Danish electricity spot price index *el*.
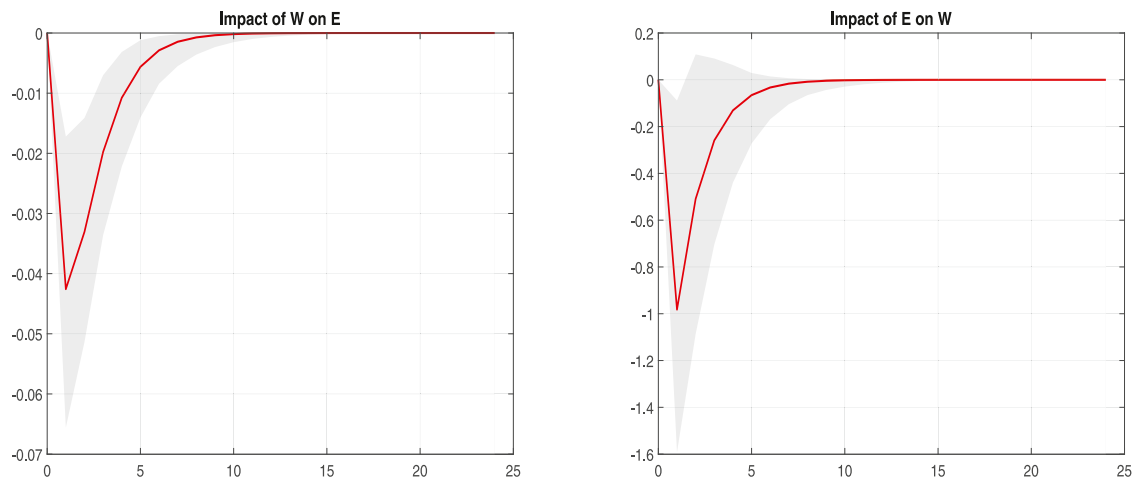
(a) Response of CO_2 emissions to wind energy   (b) Response of wind energy to CO_2 emissions

Fig. 9. Impulse-response functions from FVECM-$X_{d,b}$ including fuel and electricity prices among covariates. In gray the bootstrapped 90% confidence bands. MEA over 24 months is estimated to 0.20.

Summary statistics for the fuel and electricity price indices are given in Table 7. The two series are plotted in Fig. 8. Both are strongly persistent, more so than emissions and wind energy.

Results of including the price indices in first differences as explanatory variables in the estimation of the FVECM-$X_{d,b}$ appear in Table 8. As expected, higher wind energy is associated with lower electricity prices and emissions, whereas fuel prices enter insignificantly in this estimation. IRFs are shown in Fig. 9. MEA is now 0.20, higher than the value based on Table 4 and Fig. 5, at 0.16. This suggests that the latter estimate of the impact of wind power production on emissions is not inflated by leaving out effects operating via prices.

Most of the earlier findings for the covariates carry over. Thus, higher temperature reduces emissions, and higher precipitation and North Atlantic oscillations are associated with more wind energy production. Industrial production growth loses its significance for wind energy, which makes sense, and is consistent with the notion that electricity prices are required in the specification.

Finally, the possibility remains that a mitigating general equilibrium effect on the impact of wind power production on emissions enters via the endogeneity of prices. To examine this issue, we consider trivariate models including prices as endogenous variables. This allows testing the weak exogeneity of the price indices. Further, it allows computing IRFs between emissions and prices. This can be of interest for policy analysis. For example, turbines were subsidized in Denmark during the period under study. Subsidies can lead to more production and, e.g., export of electricity. In order to replace fossil fuels by renewables, a general tax on emissions is a better policy tool than subsidies, as it offers the decision maker a choice among alternatives, rather than steering the choice to the subsidized technology. The power of the taxation tool can potentially be investigated via IRFs with respect to prices.

Results from the trivariate model expanded with the filtered (by $\Delta^{0.6}$) world fuel price index are in Table B.8 in Appendix B.7, and those from the model expanded with filtered (by $\Delta^{0.3}$) electricity prices in Table B.9. The filtering reflects that the order of fractional integration appears about 0.6 and 0.3 higher for fuel and electricity prices, respectively, relative to emissions and wind energy. In each case, the hypothesis of weak exogeneity of the price index is not rejected. This lends support to the specification in Table 8. Still, if the possibility of endogenous electricity prices is left open, the results indicate a reduction in MEA of the order one third, to 0.11, due to the general equilibrium effect.

On the methodological side, the analysis reinforces the generality of the approach, including the feasibility of the trivariate FVECM-$X_{d,b}$, and the endogeneity tests. On the substantive side, test results indicate that the received estimates of the potential of wind energy for emissions abatement are not inflated due to left-out general equilibrium effects. Should electricity prices be endogenous, after all, the indicated mitigation effect on the abatement potential of wind energy adoption is of the order one third.

6. Conclusion

We offer an analysis of the dynamic relation between CO_2 emissions and wind energy in Denmark. As both series are strongly persistent, we pursue a fractional cointegration approach, and show that the series follow paths that are tied together in the long run. By including covariates, we are able to investigate the impact of climate and forces of demand on the potential of wind power production for emissions abatement. Local climate conditions matter for the efficiency of wind power generation. Temperature plays a dual role, as it matters for the demand for heating and cooling, as well as for efficiency in generation, through air density. From the results, the former dominates the impact on emissions, which decline as temperature increases. Wind power production increases with precipitation and North Atlantic oscillations, both of which signal stormy weather. Further demand indicators, beside temperature, include aggregate output, which matters for emissions in a manner consistent with an environmental Kuznets curve (EKC), and prices of conventional inputs (fuels) and output (power). When controlling for prices, higher wind energy is associated with lower electricity prices. Accounting for a seasonal trend, marginal CO_2 emissions avoided (MEA) per MWh of wind energy produced are estimated at 0.16 tonnes, based on impulse responses. This estimate of the abatement potential of wind power is lower than values reported in the literature, but statistically significant, and robust to including climate and demand variables. Estimated MEA is reduced by about one third by treating electricity prices as endogenous, and by one quarter by including emissions from combustion of biomass. However, formal exogeneity tests indicate that the main MEA estimate, at 0.16, is not inflated due to left-out general equilibrium effects operating via prices of conventional inputs (fossil fuels) and output (electricity) in power production. Without covariates, estimated MEA is 0.07, and insignificant.

Declaration of competing interest

The authors declare that they have no known competing financial interests or personal relationships that could have appeared to influence the work reported in this paper.

Acknowledgment

All authors have contributed equally to the article and share full responsibility for the material therein.

Appendix A. Deseasonalized data

See Fig. A.1.

Appendix B. Model specifications

B.1. FVECM$_{d,b;c}$ with no exogenous variables

See Fig. B.1 and Table B.1.

B.2. Raw data

See Fig. B.2 and Table B.2.

B.3. Two stage estimation

See Fig. B.3 and Table B.3.

(a) E_t

(b) W_t

(c) $temp_t$

(d) $precip_t$

(e) $sunshine_t$

(f) $NAOI_t$

(g) $\Delta \log(ind_t)$

(h) $(\Delta \log(ind_t))^2$
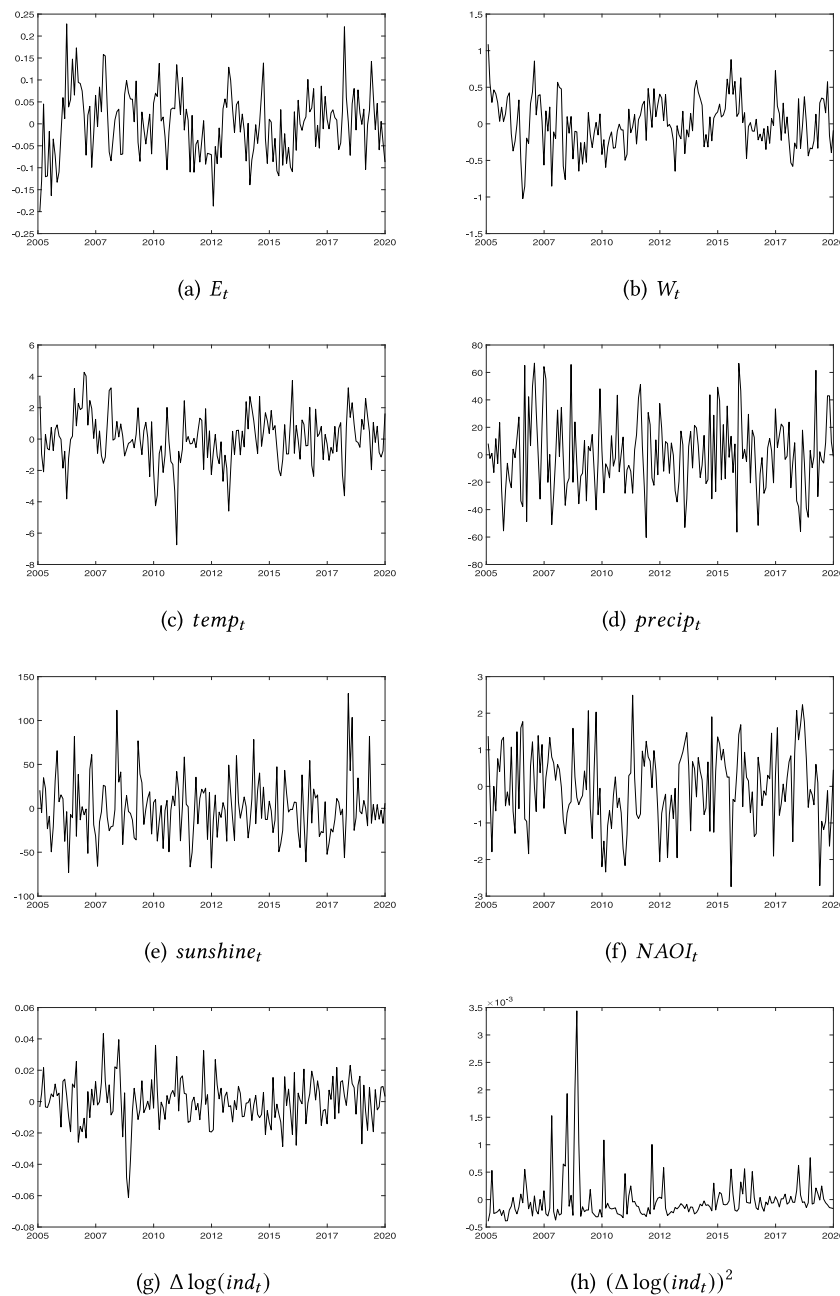
Fig. A.1. Variables used for estimation of models in deviation from trend and seasonal terms.
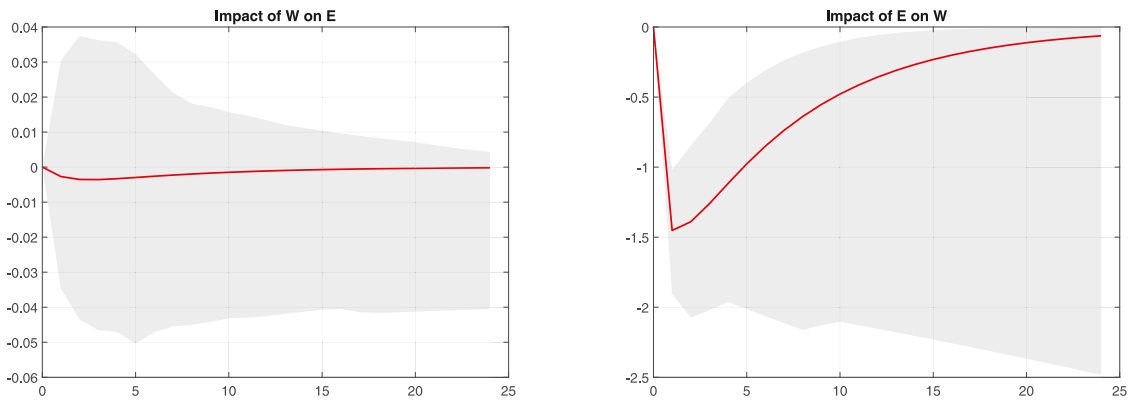
(a) Response of CO_2 emissions to wind energy   (b) Response of wind energy to CO_2 emissions

Fig. B.1. Impulse-response functions from FVECM. In gray the bootstrapped 90% confidence bands. MEA over 24 months is estimated to 0.0713.
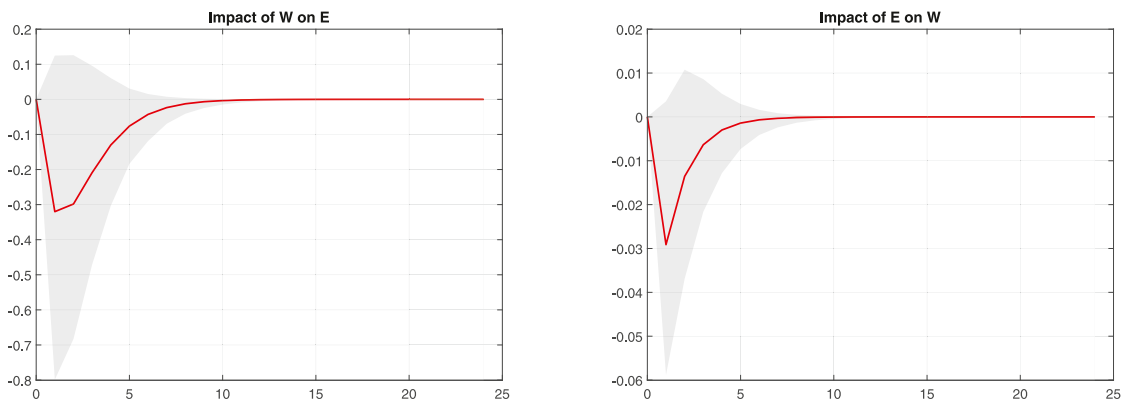
(a) Response of CO_2 emissions to wind energy   (b) Response of wind energy to CO_2 emissions

Fig. B.2. Impulse-response functions from FVECM-X$_{d,b}$ using raw data. In gray the bootstrapped 90% confidence bands. MEA over 24 months is estimated to 0.0852.
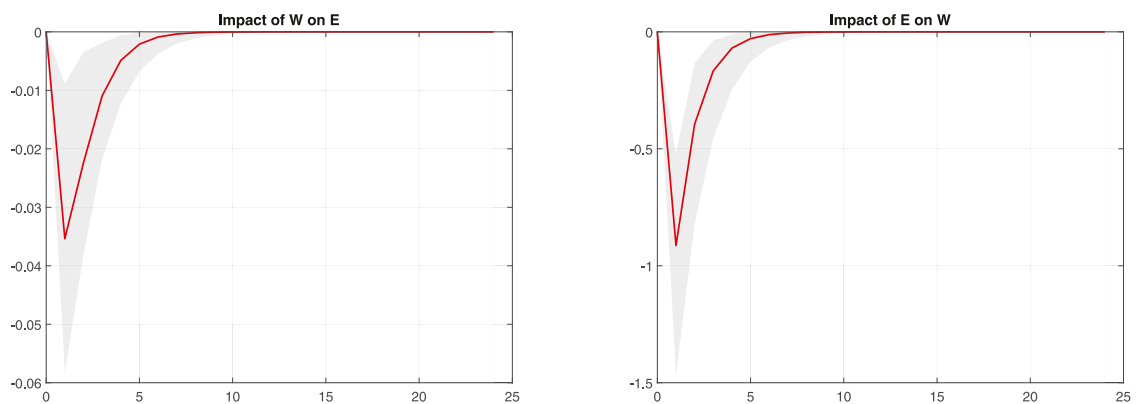
(a) Response of CO_2 emissions to wind energy   (b) Response of wind energy to CO_2 emissions

Fig. B.3. Impulse-response functions from FVECM-X$_{d,b}$ with two step procedure. In gray the bootstrapped 90% confidence bands. MEA over 24 months is estimated to 0.1387.

Table B.1
FVECM results. The table reports the results of estimation of the FVECM using the monthly emissions and wind energy series E_t and W_t over the period January, 2005, through December, 2019. The Johansen and Nielsen (2012) rank test indicates fractional cointegration with $r = 1$ (LR = 17.893 for $r = 0$, LR = 3.263 for $r = 1$). The estimated cointegration vector for $r = 1$ is $\hat{\beta} = (1.0000, 0.2581)$. The bottom lines report Ljung–Box (LB) tests for five and ten periods, the associated p-values, and the Doornik and Hansen (2008) test of multivariate normality. The maximized value of the log-likelihood function is 121.762. The lag length is $k = 1$, as selected by BIC, and the LR test of $k = 0$ gets p-value 0.0015. MEA is estimated to 0.0713, with bootstrap confidence interval at 90% given by $(-0.6877, 1.0412)$.

	E_t				W_t			
	Est.	Std.Err.	t-stat	p-val	Est.	Std.Err.	t-stat	p-val
Estimates								
d	0.8136	0.1219	6.6737	0.0000	0.8136	0.1219	6.6737	0.0000
α	−0.1377	0.0837	−1.6454	0.0999	−0.7187	0.2311	−3.1105	0.0019
β	1.0000	–	–	–	0.2581	0.0389	6.6339	0.0000
μ	8.3692	0.0751	111.3707	0.0000	−1.3171	0.2789	−4.7223	0.0000
$\Gamma_{1,:}$	0.0787	0.0608	1.2945	0.1955	0.0130	0.0094	1.3850	0.1661
$\Gamma_{2,:}$	−0.1396	0.1300	−1.0736	0.2830	−0.1093	0.0349	−3.1316	0.0017
Misspecification tests								
LB(5)	42.8612	–	–	0.0000	6.7062	–	–	0.2434
LB(10)	128.0273	–	–	0.0000	12.8876	–	–	0.2300
Normality	12.7601	–	–	0.0125				

Table B.2
FVECM-X$_{d,b}$ results using raw data. The table reports the results of estimation of the FVECM-X$_{d,b}$ using the original monthly emissions (CO_2) and wind energy ($Wind$) series over the period January, 2005, through December, 2019. The Johansen and Nielsen (2012) rank test indicates fractional cointegration with $r = 1$ (LR = 5.2089 for $r = 0$, LR = 2.2562 for $r = 1$). The estimated cointegration vector for $r = 1$ is $\hat{\beta} = (1.0000, 4.279)$. The bottom lines report Ljung–Box (LB) tests for five and ten periods, the associated p-values, and the Doornik and Hansen (2008) test of multivariate normality. The maximized value of the log-likelihood function is 280.942. MEA is estimated to 0.0852, with bootstrap confidence interval at 90% given by $(-0.0379, 0.1799)$.

|	CO_2				$Wind_t$			
	Est.	Std.Err.	t-stat	p-val	Est.	Std.Err.	t-stat	p-val
Estimates								
d	0.4985	0.0621	8.0296	0.0000	0.4985	0.0621	8.0296	0.0000
α	−0.1561	0.0843	−1.8509	0.0642	0.0060	0.0232	0.2604	0.7945
β	1.0000	–	–	–	4.2790	2.7971	1.5298	0.1261
μ	4.5927	0.1606	28.6014	0.0000	0.1912	0.0418	4.5698	0.0000
$trend$	−0.0102	0.0018	−5.7683	0.0000	0.0020	0.0005	4.5169	0.0000
$\sin(2\pi t/12)$	−0.1700	0.0795	−2.1393	0.0324	−0.0117	0.0181	−0.6479	0.5171
$\cos(2\pi t/12)$	0.1877	0.0977	1.9198	0.0549	−0.0278	0.0221	−1.2584	0.2082
$temp$	−0.4955	0.0816	−6.0739	0.0000	0.0030	0.0184	0.1620	0.8713
$precip$	−0.0148	0.0244	−0.6046	0.5455	0.0185	0.0054	3.4388	0.0006
$sunshine$	0.0915	0.0524	1.7449	0.0810	−0.0036	0.0116	−0.3140	0.7535
$NAOI$	−0.0345	0.0217	−1.5898	0.1119	0.0095	0.0048	1.9733	0.0485
$\Delta \log(ind)$	0.0104	0.0194	0.5384	0.5903	−0.0168	0.0043	−3.9115	0.0001
$[\Delta \log(ind)]^2$	0.0351	0.0191	1.8372	0.0662	0.0014	0.0043	0.3273	0.7435
Misspecification tests								
LB(5)	14.4687	–	–	0.0129	5.1168	–	–	0.4018
LB(10)	18.4732	–	–	0.0475	17.2946	–	–	0.0681
Normality	13.4131	–	–	0.0094				

Table B.3
FVECM results using residuals. The table reports the results of estimation of the FVECM using the residuals from the regressions of the monthly emissions and wind energy series E_t and W_t on the covariate specification μ_t from (2) over the period January, 2005, through December, 2019. The Johansen and Nielsen (2012) rank test indicates fractional cointegration with $r = 1$ (LR = 11.151 for $r = 0$, LR = 0.9021 for $r = 1$). The estimated cointegration vector for $r = 1$ is $\hat{\beta} = (1.0000, 0.2866)$. The bottom lines report Ljung–Box (LB) tests for five and ten periods, the associated p-values, and the Doornik and Hansen (2008) test of multivariate normality. The maximized value of the log-likelihood function is 245.563. MEA is estimated to 0.1387, with bootstrap confidence interval at 90% given by $(0.0229, 0.2174)$.

	$Y_{1,t}$				$Y_{2,t}$			
Estimates								
d	0.4120	0.0632	6.5205	0.0000	0.4120	0.0632	6.5205	0.0000
α	−0.3292	0.1125	−2.9269	0.0034	−0.4690	0.6382	−0.7349	0.4624
β	1.0000	–	–	–	0.2866	0.0694	4.1274	0.0000
μ	−0.0341	0.0296	−1.1506	0.2499	0.1414	0.1171	1.2078	0.2271
Misspecification tests								
LB(5)	16.2438	–	–	0.0062	1.2053	–	–	0.9444
LB(10)	19.0000	–	–	0.0403	14.7352	–	–	0.1420
Normality	2.2580	–	–	0.6884				

Table B.4

FVECM-X$_{d,b}$ results imposing $\alpha_2 = 0$. The table reports the results of estimation of the FVECM-X$_{d,b}$ using the monthly emissions and wind energy series E_t and W_t over the period January, 2005, through December, 2019. The restriction $\alpha_2 = 0$ is imposed. The Johansen and Nielsen (2012) rank test indicates fractional cointegration with $r = 1$ (LR = 11.5778 for $r = 0$, LR = 0.7819 for $r = 1$). The estimated cointegration vector is $\hat{\beta} = (1.0000, 0.2667)$. The bottom lines report Ljung-Box (LB) tests for five and ten periods, the associated p-values, and the Doornik and Hansen (2008) test of multivariate normality. The maximized value of the log-likelihood function is 250.160. MEA is estimated to 0.1645, with bootstrap confidence interval at 90% given by (0.0571,0.2347).

	E_t				W_t			
	Est.	Std.Err.	t-stat	p-val	Est.	Std.Err.	t-stat	p-val
Estimates								
d	0.4377	0.0540	8.1098	0.0000	0.4377	0.0540	8.1098	0.0000
α	−0.3593	0.1023	−3.5125	0.0004	0.0000	–	–	–
β	1.0000	–	–	–	0.2667	0.0770	3.4636	0.0005
μ	8.4281	0.0359	234.4486	0.0000	0.2662	0.0548	4.8577	0.0000
$trend$	−0.0026	0.0004	−6.7994	0.0000	0.0104	0.0017	6.0206	0.0000
$\sin(2\pi t/12)$	−0.0287	0.0192	−1.4959	0.1347	−0.0511	0.0917	−0.5573	0.5773
$\cos(2\pi t/12)$	0.0623	0.0236	2.6344	0.0084	−0.1266	0.1130	−1.1199	0.2627
$temp$	−0.1096	0.0199	−5.5014	0.0000	0.0093	0.0944	0.0981	0.9219
$precip$	−0.0048	0.0060	−0.7891	0.4301	0.0943	0.0283	3.3276	0.0009
$sunshine$	0.0183	0.0130	1.4101	0.1585	−0.0158	0.0609	−0.2594	0.7954
$NAOI$	−0.0068	0.0053	−1.2749	0.2023	0.0594	0.0252	2.3604	0.0183
$\Delta\log(ind)$	0.0039	0.0047	0.8299	0.4066	−0.0916	0.0223	−4.1080	0.0000
$[\Delta\log(ind)]^2$	0.0069	0.0047	1.4837	0.1379	−0.0107	0.0221	−0.4833	0.6289
Misspecification tests								
LB(5)	17.5275	–	–	0.0036	1.9334	–	–	0.8583
LB(10)	19.5927	–	–	0.0333	15.9917	–	–	0.0999
Normality	1.3278	–	–	0.8566				
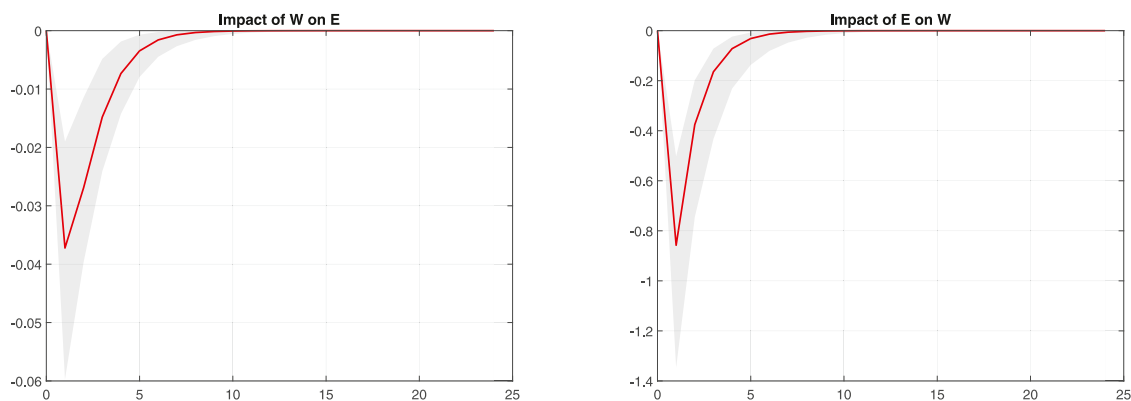
(a) Response of CO$_2$ emissions to wind energy   (b) Response of wind energy to CO$_2$ emissions

Fig. B.4. Impulse-response functions from FVECM-X$_{d,b}$ model with $\alpha_2 = 0$. In gray the bootstrapped 90% confidence bands. MEA over 24 months is estimated to 0.1645.

B.4. Weak exogeneity of W_t

See Fig. B.4 and Table B.4.

B.5. Sensitivity to emissions measure

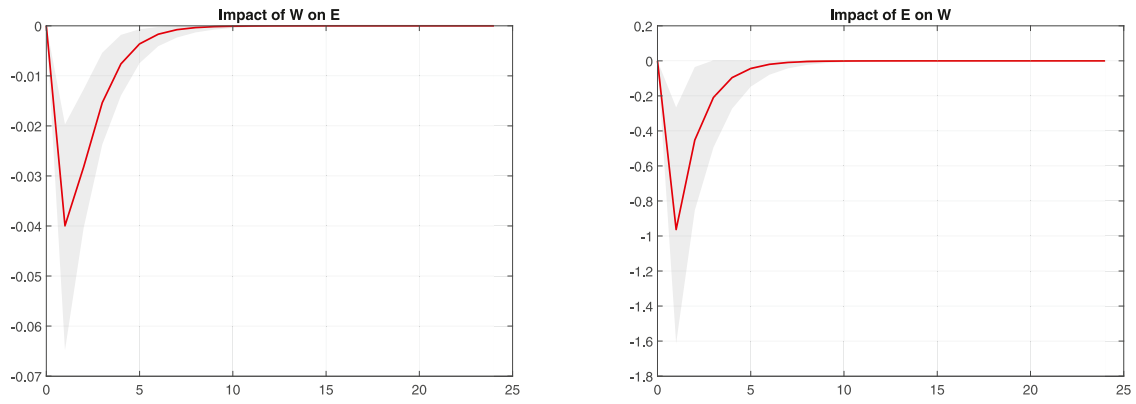See Figs. B.5 and B.6 and Tables B.5 and B.6.

B.6. Long-term forecasting

See Figs. B.7 and B.8 and Table B.7.

B.7. Input and output prices

See Figs. B.9 and B.10 and Tables B.8 and B.9.

Appendix C. Supplementary data

Supplementary material related to this article can be found online at https://doi.org/10.1016/j.eneco.2023.106821.

(a) Response of CO_2 emissions to wind energy   (b) Response of wind energy to CO_2 emissions

Fig. B.5. Impulse-response functions from FVECM-X$_{d,b}$ model without CO_2 from waste. In gray the bootstrapped 90% confidence bands. MEA over 24 months is estimated to 0.1736.
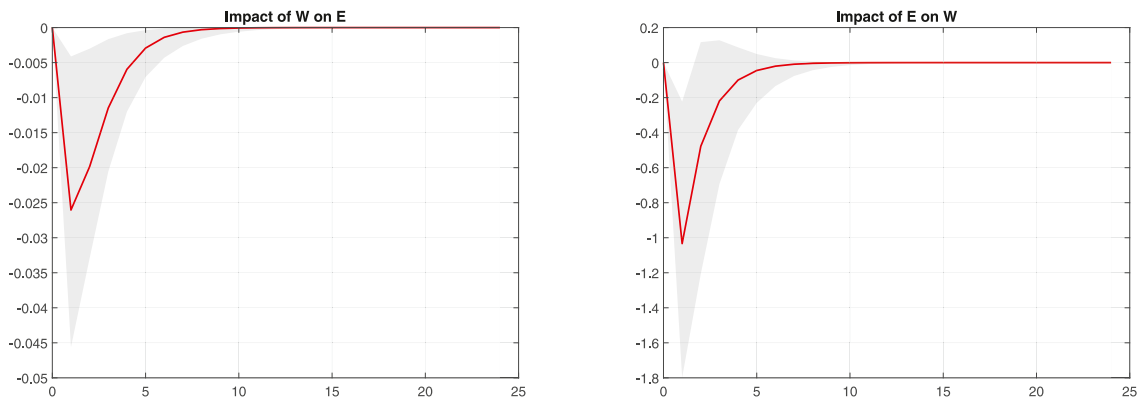
(a) Response of CO_2 emissions to wind energy   (b) Response of wind energy to CO_2 emissions

Fig. B.6. Impulse-response functions from FVECM-X$_{d,b}$ model with biomass. In gray the bootstrapped 90% confidence bands. MEA over 24 months is estimated to 0.1222.

(a) Response of CO_2 emissions to wind energy   (b) Response of wind energy to CO_2 emissions

Fig. B.7. Impulse-response functions from VAR(2) model with deterministic terms. In gray the bootstrapped 90% confidence bands. MEA over 24 months is estimated to 0.0750.

Table B.5

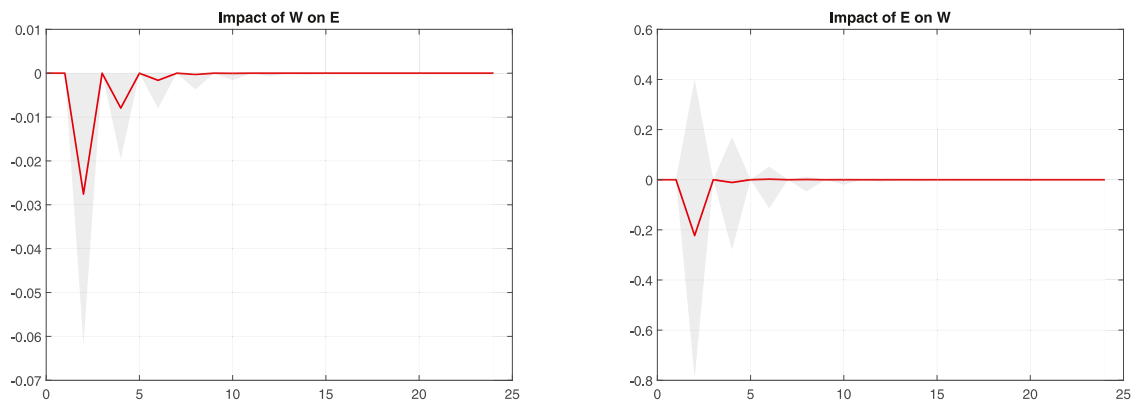FVECM-X$_{d,b}$ results excluding emissions from waste burning. The table reports the results of estimation of the FVECM-X$_{d,b}$ using the monthly CO$_2$ emissions series E_t (excluding emissions from waste burning) and wind energy series W_t over the period January, 2005, through December, 2019. The Johansen and Nielsen (2012) rank test indicates fractional cointegration with $r = 1$ (LR = 13.0002 for $r = 0$, LR = 0.6723 for $r = 1$). The estimated cointegration vector for $r = 1$ is $\hat{\beta} = (1.0000, 0.2746)$. The bottom lines report Ljung–Box (LB) tests for five and ten periods, the associated p-values, and the Doornik and Hansen (2008) test of multivariate normality. The maximized value of the log-likelihood function is 249.644. MEA is estimated to 0.1736, with bootstrap confidence interval at 90% given by (0.0781,0.2741).

	E_t				W_t			
	Est.	Std.Err.	t-stat	p-val	Est.	Std.Err.	t-stat	p-val
Estimates								
d	0.4526	0.0628	7.2047	0.0000	0.4526	0.0628	7.2047	0.0000
α	−0.3522	0.1040	−3.3866	0.0007	−0.3152	0.6327	−0.4982	0.6183
β	1.0000	–	–	–	0.2746	0.0690	3.9783	0.0001
μ	8.4275	0.0381	221.1002	0.0000	−1.6086	0.1639	−9.8166	0.0000
$trend$	−0.0027	0.0004	−6.7365	0.0000	0.0104	0.0017	6.2157	0.0000
$\sin(2\pi t/12)$	−0.0283	0.0193	−1.4664	0.1425	−0.0424	0.0930	−0.4555	0.6488
$\cos(2\pi t/12)$	0.0641	0.0238	2.6905	0.0071	−0.1186	0.1140	−1.0397	0.2985
$temp$	−0.1097	0.0200	−5.4787	0.0000	0.0187	0.0961	0.1946	0.8457
$precip$	−0.0046	0.0061	−0.7593	0.4477	0.0948	0.0284	3.3372	0.0008
$sunshine$	0.0187	0.0130	1.4317	0.1522	−0.0171	0.0611	−0.2793	0.7800
$NAOI$	−0.0070	0.0054	−1.3023	0.1928	0.0596	0.0252	2.3689	0.0178
$\Delta\log(ind)$	0.0041	0.0048	0.8627	0.3883	−0.0906	0.0224	−4.0518	0.0001
$[\Delta\log(ind)]^2$	0.0065	0.0047	1.3764	0.1687	−0.0110	0.0220	−0.4988	0.6179
Misspecification tests								
LB(5)	16.9580	–	–	0.0046	1.9044	–	–	0.8622
LB(10)	18.8572	–	–	0.0421	16.3114	–	–	0.0911
Normality	1.1779	–	–	0.8817				

Table B.6

FVECM-X$_{d,b}$ results with emissions from biomass. The table reports the results of estimation of the FVECM-X$_{d,b}$ using the monthly CO$_2$ emissions series E_t (including emissions from the combustion of biomass) and wind energy series W_t over the period January, 2005, through December, 2019. The Johansen and Nielsen (2012) rank test indicates fractional cointegration with $r = 1$ (LR = 8.3516 for $r = 0$, LR = 1.2577 for $r = 1$). The estimated cointegration vector for $r = 1$ is $\hat{\beta} = (1.0000, 0.2763)$. The bottom lines report Ljung–Box (LB) tests for five and ten periods, the associated p-values, and the Doornik and Hansen (2008) test of multivariate normality. The maximized value of the log-likelihood function is 263.609. MEA is estimated to 0.1222, with bootstrap confidence interval at 90% given by (0.0103,0.2212).

	E_t				W_t			
	Est.	Std.Err.	t-stat	p-val	Est.	Std.Err.	t-stat	p-val
Estimates								
d	0.4489	0.0617	7.2755	0.0000	0.4489	0.0617	7.2755	0.0000
α	−0.2307	0.0910	−2.5362	0.0112	−0.2466	0.6122	−0.4028	0.6871
β	1.0000	–	–	–	0.2763	0.0681	4.0573	0.0001
μ	8.4747	0.0351	241.7878	0.0000	−1.6397	0.1650	−9.9387	0.0000
$trend$	−0.0020	0.0004	−5.2966	0.0000	0.0106	0.0016	6.4196	0.0000
$\sin(2\pi t/12)$	−0.0306	0.0179	−1.7123	0.0868	−0.0454	0.0935	−0.4860	0.6269
$\cos(2\pi t/12)$	0.0481	0.0220	2.1805	0.0292	−0.1202	0.1147	−1.0478	0.2947
$temp$	−0.1024	0.0185	−5.5407	0.0000	0.0139	0.0966	0.1437	0.8858
$precip$	−0.0065	0.0056	−1.1729	0.2408	0.0944	0.0286	3.3053	0.0009
$sunshine$	0.0165	0.0120	1.3795	0.1678	−0.0144	0.0614	−0.2344	0.8147
$NAOI$	−0.0078	0.0049	−1.5814	0.1138	0.0584	0.0254	2.3019	0.0213
$\Delta\log(ind)$	0.0049	0.0044	1.1087	0.2675	−0.0923	0.0225	−4.0968	0.0000
$[\Delta\log(ind)]^2$	0.0065	0.0044	1.4949	0.1349	−0.0102	0.0223	−0.4593	0.6460
Misspecification tests								
LB(5)	16.2654	–	–	0.0061	1.9282	–	–	0.8590
LB(10)	18.2968	–	–	0.0502	16.4303	–	–	0.0880
Normality	1.9788	–	–	0.7397				

Table B.7

VAR results. The table reports the results of estimation of the VAR(2) model with deterministic terms using the monthly emissions and wind energy series E_t and W_t over the period January, 2005, through December, 2019. The bottom lines report Ljung–Box (LB) tests for five and ten periods, the associated p-values, and the Doornik and Hansen (2008) test of multivariate normality. MEA is estimated to 0.0750.

|	E_t				W_t			
	Est.	Std.Err.	t-stat	p-val	Est.	Std.Err.	t-stat	p-val
Estimates								
E_{t-1}	0.2237	0.1808	1.2369	0.2161	−0.0327	0.0178	−1.8397	0.0658
W_{t-1}	−0.3222	0.3979	−0.8096	0.4182	0.3140	0.1809	1.7353	0.0827
E_{t-2}	0.0849	0.0974	0.8719	0.3833	−0.0311	0.0197	−1.5775	0.1147
W_{t-2}	0.2240	0.3951	0.5669	0.5708	0.2036	0.0874	2.3298	0.0198
μ	8.4845	0.0229	370.3726	0.0000	−1.8894	0.1185	−15.9432	0.0000
$trend$	−0.0029	0.0002	−13.5924	0.0000	0.0121	0.0011	11.3598	0.0000
$\sin(2\pi t/12)$	0.0670	0.0101	6.6095	0.0000	−0.1153	0.0479	−2.4077	0.0161
$\cos(2\pi t/12)$	0.1470	0.0101	14.5984	0.0000	−0.0567	0.0474	−1.1966	0.2314
Misspecification tests								
LB(5)	4.5291	–	–	0.4760	2.9510	–	–	0.7075
LB(10)	7.0189	–	–	0.7237	7.5164	–	–	0.6760
Normality	4.4493	–	–	0.3486				

(a) Forecast of E_t

(b) Forecast of W_t
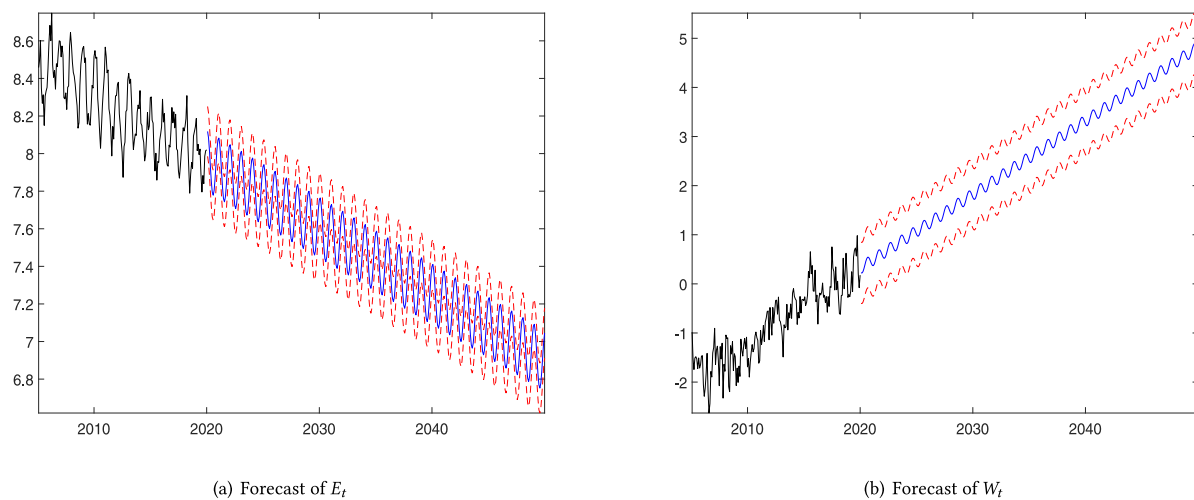
Fig. B.8. Long-term forecasts of E_t and W_t based on the VAR(2) with deterministic terms. In red the 95% confidence band. In black the observed series.

Table B.8

Trivariate FVECM-X$_{d,b}$ with filtered fuel price index. The table reports results of the estimation of the trivariate FVECM-X$_{d,b}$ with filtered fuel price index using the monthly emissions (CO$_2$), fuel price, and wind energy series E_t, $\Delta^{0.6}fuel_t$, and W_t over the period January, 2005, through December, 2019. The Johansen and Nielsen (2012) rank test indicates fractional cointegration with $r = 2$ (LR = 21.309 for $r = 0$, LR = 5.377 for $r = 1$, LR = 1.178 for $r = 2$). The estimated cointegration vectors for $r = 2$ are $\hat{\beta}'_1 = (1.0000, 0.0000, 0.2456)$ and $\hat{\beta}'_2 = (0.0000, 1.0000, 0.4846)$. The bottom lines report Ljung–Box (LB) tests for five and ten periods, the associated p-values, and the Doornik and Hansen (2008) test of multivariate normality. The maximized value of the log-likelihood function is 497.424. MEA is estimated to 0.1928, with bootstrap confidence interval at 90% given by (0.0818,0.3142). The Wald test of the null of weak exogeneity of fuel prices, $(\alpha_{fuel,1}, \alpha_{fuel,2})' = 0$, takes the value 1.0897 (p-value 0.5799).

|	E_t				$\Delta^{0.6}fuel_t$				W_t			
	Est.	Std.Err.	t-stat	p-val	Est.	Std.Err.	t-stat	p-val	Est.	Std.Err.	t-stat	p-val
Estimates												
d	0.5883	0.0629	9.3461	0.0000	0.5883	0.0629	9.3461	0.0000	0.5883	0.0629	9.3461	0.0000
α_1	−0.4649	0.1085	−4.2840	0.0000	0.0455	0.1208	0.3762	0.7068	−0.1183	0.5529	−0.2140	0.8305
α_2	0.0832	0.0477	1.7430	0.0813	−0.0595	0.0488	−1.2202	0.2224	−0.4634	0.2359	−1.9647	0.0495
μ	8.4284	0.0305	276.0004	0.0000	−0.0481	0.0502	−0.9590	0.3376	−1.6255	0.1404	−11.5785	0.0000
$trend$	−0.0025	0.0004	−7.1055	0.0000	0.0002	0.0006	0.2769	0.7819	0.0104	0.0016	6.5610	0.0000
$\sin(2\pi t/12)$	−0.0270	0.0197	−1.3729	0.1698	0.0023	0.0209	0.1079	0.9141	−0.0529	0.0940	−0.5632	0.5733
$\cos(2\pi t/12)$	0.0641	0.0240	2.6755	0.0075	−0.0093	0.0252	−0.3711	0.7105	−0.1271	0.1147	−1.1075	0.2681
$temp$	−0.1081	0.0201	−5.3656	0.0000	−0.0030	0.0210	−0.1448	0.8849	0.0071	0.0962	0.0740	0.9410
$precip$	−0.0043	0.0060	−0.7192	0.4720	0.0009	0.0061	0.1492	0.8814	0.0960	0.0283	3.3907	0.0007
$sunshine$	0.0189	0.0129	1.4571	0.1451	0.0148	0.0132	1.1260	0.2602	−0.0164	0.0609	−0.2691	0.7878
$NAOI$	−0.0068	0.0053	−1.2800	0.2005	0.0081	0.0055	1.4754	0.1401	0.0599	0.0252	2.3745	0.0176
$\Delta\log(ind)$	0.0036	0.0048	0.7516	0.4523	0.0266	0.0051	5.2320	0.0000	−0.0862	0.0231	−3.7328	0.0002
$[\Delta\log(ind)]^2$	0.0066	0.0048	1.3968	0.1625	−0.0108	0.0049	−2.1988	0.0279	−0.0122	0.0228	−0.5352	0.5925
Misspecification tests												
LB(5)	18.1072	–	–	0.0028	2.5239	–	–	0.7729	2.1816	–	–	0.8235
LB(10)	20.2186	–	–	0.0273	11.2181	–	–	0.3408	15.7804	–	–	0.1061
Normality	10.4333	–	–	0.1075								
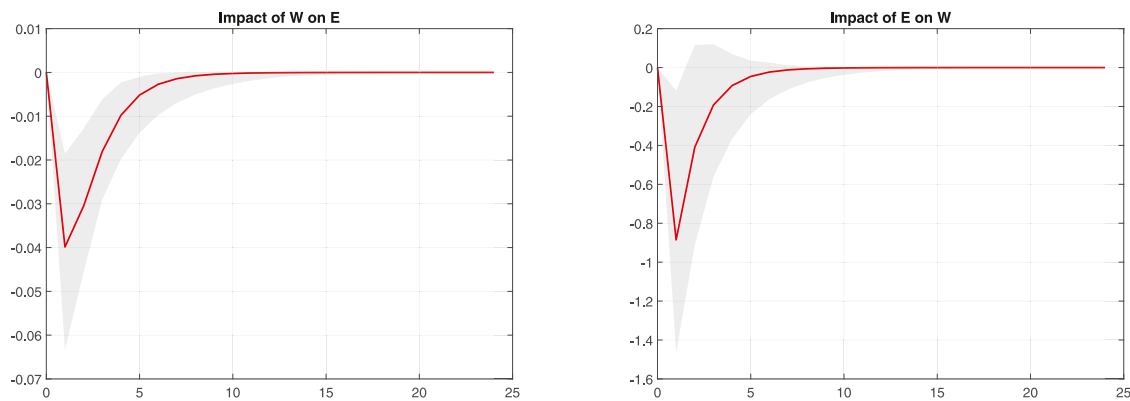
(a) Response of CO_2 emissions to wind energy   (b) Response of wind energy to CO_2 emissions

Fig. B.9. Impulse-response functions of CO_2 emissions and wind energy from the trivariate FVECM-X$_{d,b}$ with filtered fuel price index. In gray the bootstrapped 90% confidence bands. MEA over 24 months is estimated to 0.1928.

Table B.9

Trivariate FVECM-X$_{d,b}$ with filtered electricity prices. The table reports the results of estimation of the trivariate FVECM-X$_{d,b}$ with filtered electricity prices using the monthly emissions (CO_2), electricity price, and wind energy series E_t, $\Delta^{0.6} el_t$ and W_t over the period January, 2005, through December, 2019. The Johansen and Nielsen (2012) rank test indicates fractional cointegration with $r = 2$ (LR = 25.960 for $r = 0$, LR = 9.033 for $r = 1$, LR = 2.113 for $r = 2$). The estimated cointegration vectors for $r = 2$ are $\hat{\beta}_1' = (1.0000, 0.0000, 0.2351)$ and $\hat{\beta}_2' = (0.0000, 1.0000, 0.6719)$. The bottom lines report Ljung–Box (LB) tests for five and ten periods, the associated p-values, and the Doornik and Hansen (2008) test of multivariate normality. The maximized value of the log-likelihood function is 428.251. MEA is estimated to 0.1112, with bootstrap confidence interval at 90% given by (0.0330,0.2900). The Wald test of the null of weak exogeneity of electricity prices, $(\alpha_{el,1}, \alpha_{el,2})' = 0$, takes the value 1.4558 (p-value 0.4853).

	E_t				$\Delta^{0.3} el_t$				W_t			
	Est.	Std.Err.	t-stat	p-val	Est.	Std.Err.	t-stat	p-val	Est.	Std.Err.	t-stat	p-val
Estimates												
d	0.5849	0.0616	9.4974	0.0000	0.5849	0.0616	9.4974	0.0000	0.5849	0.0616	9.4974	0.0000
α_1	−0.4816	0.1107	−4.3487	0.0000	0.0204	0.2106	0.0966	0.9230	0.1683	0.5652	0.2978	0.7659
α_2	0.0748	0.0398	1.8779	0.0604	0.0744	0.0764	0.9738	0.3302	−0.5792	0.1911	−3.0316	0.0024
μ	8.4291	0.0322	261.8015	0.0000	−0.0850	0.0909	−0.9352	0.3497	−1.6319	0.1405	−11.6161	0.0000
$trend$	−0.0025	0.0004	−5.9132	0.0000	0.0008	0.0012	0.6124	0.5403	0.0104	0.0019	5.5936	0.0000
$\sin(2\pi t/12)$	−0.0272	0.0196	−1.3904	0.1644	−0.1873	0.0338	−5.5452	0.0000	−0.0619	0.0935	−0.6621	0.5079
$\cos(2\pi t/12)$	0.0656	0.0242	2.7125	0.0067	−0.0864	0.0409	−2.1132	0.0346	−0.1683	0.1149	−1.4638	0.1432
$temp$	−0.1083	0.0201	−5.3956	0.0000	−0.1267	0.0336	−3.7650	0.0002	−0.0041	0.0955	−0.0425	0.9661
$precip$	−0.0040	0.0060	−0.6657	0.5056	−0.0163	0.0098	−1.6716	0.0946	0.0936	0.0281	3.3349	0.0009
$sunshine$	0.0196	0.0129	1.5163	0.1294	0.0092	0.0209	0.4390	0.6607	−0.0329	0.0608	−0.5404	0.5889
$NAOI$	−0.0074	0.0053	−1.3866	0.1656	−0.0117	0.0088	−1.3282	0.1841	0.0660	0.0250	2.6427	0.0082
$\Delta \log(ind)$	0.0050	0.0049	1.0107	0.3121	0.0842	0.0079	10.7080	0.0000	−0.1087	0.0233	−4.6617	0.0000
$[\Delta \log(ind)]^2$	0.0057	0.0047	1.2244	0.2208	0.0178	0.0078	2.2646	0.0235	−0.0044	0.0219	−0.2010	0.8407
Misspecification tests												
LB(5)	19.0622	–	–	0.0019	0.5568	–	–	0.9899	1.8582	–	–	0.8684
LB(10)	20.9494	–	–	0.0214	4.1951	–	–	0.9381	18.5798	–	–	0.0459
Normality	21.5205	–	–	0.0015								
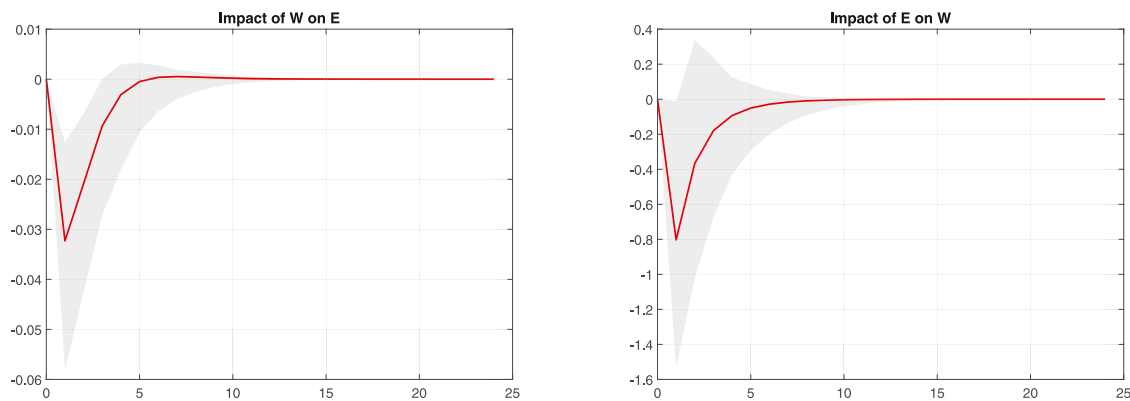
(a) Response of CO_2 emissions to wind energy   (b) Response of wind energy to CO_2 emissions

Fig. B.10. Impulse-response functions of CO_2 emissions and wind energy from the trivariate FVECM-X$_{d,b}$ with filtered electricity price index. In gray the bootstrapped 90% confidence bands. MEA over 24 months is estimated to 0.1112.

References

Abrell, J., Kosch, M., Rausch, S., 2019. Carbon abatement with renewables: Evaluating wind and solar subsidies in Germany and Spain. J. Public Econ. 169, 172–202.

Amor, M.B., de Villemeur, E.B., Pellat, M., Pineau, P.-O., 2014. Influence of wind power on hourly electricity prices and GHG (greenhouse gas) emissions: Evidence that congestion matters from Ontario zonal data. Energy 66, 458–469.

Cappelen, J., 2018. Denmark: DMI Historical Climate Data Collection 1768-2017. Danish Meteorological Institute.

Cappelen, J., Jørgensen, B., 2011. Dansk Vejr Siden 1874–Måned for Måned Med Temperatur, Nedbør og Soltimer Samt Beskrivelser af Vejret - with English Translations. Technical Report 11-02, DMI Teknisk Rapport.

Carlini, F., Santucci de Magistris, P., 2019a. On the identification of fractionally cointegrated VAR models with the $F(d)$ condition. J. Bus. Econom. Statist. 37, 135–146.

Carlini, F., Santucci de Magistris, P., 2019b. Resuscitating the Co-Fractional Model of Granger 1986. Technical report, CREATES WP series.

Christensen, B.J., Datta Gupta, N., Santucci de Magistris, P., 2021. Measuring the impact of clean energy production on CO_2 abatement in Denmark: Upper bound estimation and forecasting. J. R. Statist. Soc. Ser. A 184 (1), 118–149.

Clancy, M., Gaffney, F., 2014. Quantifying Ireland's Fuel and CO_2 Emissions Savings from Renewable Electricity in 2012. Technical report, Sustainable Energy Authority of Ireland.

Corbetta, G., Ho, A., Pineda, I., 2015. Wind Energy Scenarios for 2030. Technical report, Report by the European Wind Energy Association.

Cullen, J., 2013. Measuring the environmental benefits of wind-generated electricity. Am. Econ. J. Econ. Policy 5 (4), 107–133.

Davidson, J., 2002. A model of fractional cointegration, and tests for cointegration using the bootstrap. J. Econometrics 110 (2), 187–212.

Di Cosmo, V., Valeri, L.M., 2018a. How much does wind power reduce CO_2 emissions? Evidence from the Irish single electricity market. Environ. Resour. Econ. 71 (3), 645–669.

Di Cosmo, V., Valeri, L.M., 2018b. Wind, storage, interconnection and the cost of electricity generation. Energy Econ. 69, 1–18.

Doornik, J.A., Hansen, H., 2008. An omnibus test for univariate and multivariate normality. Oxf. Bull. Econ. Stat. 70, 927–939.

Granger, C.W.J., 1986. Developments in the study of cointegrated economic variables. Oxf. Bull. Econ. Stat. 48 (3), 213–228.

Grossman, G.M., Krueger, A.B., 1995. Economic growth and the environment. Q. J. Econ. 110 (2), 353–377.

GWEC, 2016. Global Wind Energy Outlook 2016. Technical report, Global Wind Energy Council.

Hanna, E., Cappelen, J., Allan, R., Jónsson, T., Le Blancq, F., Lillington, T., Hickey, K., 2008. New insights into North European and North Atlantic surface pressure variability, storminess, and related climatic change since 1830. J. Clim. 21 (24), 6739–6766.

Hernandez, C.V., Gonzalez, J.S., Fernandez-Blanco, R., 2019. New method to assess the long-term role of wind energy generation in reduction of CO_2 emissions–case study of the European union. J. Clean. Prod. 207, 1099–1111.

Holtz-Eakin, D., Selden, T.M., 1995. Stoking the fires? CO_2 emissions and economic growth. J. Public Econ. 57 (1), 85–101.

IPCC, 2019. Global Warming of 1.5 °C. Technical report, Intergovernmental Panel on Climate Change.

Jacobson, M.Z., Delucchi, M.A., 2011. Providing all global energy with wind, water, and solar power, part I: Technologies, energy resources, quantities and areas of infrastructure, and materials. Energy Policy 39 (3), 1154–1169.

Johansen, S., 1991. Estimation and hypothesis testing of cointegration vectors in Gaussian vector autoregressive models. Econometrica 56, 1551–1580.

Johansen, S., 1992. Testing weak exogeneity and the order of cointegration in UK money demand data. J. Policy Model. 14 (3), 313–334.

Johansen, S., 1995. Likelihood-Based Inference in Cointegrated Vector Autoregressive Models. Oxford University Press, Oxford.

Johansen, S., 2008. A representation theory for a class of vector autoregressive models for fractional processes. Econom. Theory 24 (3), 651–676.

Johansen, S., Nielsen, M.Ø., 2012. Likelihood inference for a fractionally cointegrated vector autoregressive model. Econometrica 80 (6), 2667–2732.

Kaffine, D.T., McBee, B.J., Lieskovsky, J., 2013. Emissions savings from wind power generation in Texas. Energy J. 34 (1), 155–175.

Leduc, M., Matthews, H.D., de Elía, R., 2016. Regional estimates of the transient climate response to cumulative CO_2 emissions. Nature Clim. Change 6 (5), 474–478.

Newey, W.K., West, K.D., 1987. A simple, positive semi-definite, heteroskedasticity and autocorrelation consistent covariance matrix. Econometrica 55 (3), 703–708.

Nielsen, M.Ø., Popiel, M.K., 2018. A Matlab Program and User's Guide for the Fractionally Cointegrated VAR Model. Technical report, Queen's Economics Department Working Paper.

Nielsen, M.Ø., Shibaev, S.S., 2018. Forecasting daily political opinion polls using the fractionally cointegrated vector auto-regressive model. J. R. Stat. Soc. Ser. A 181 (1), 3–33.

Nielsen, O.-K., et al., 2016. Denmark's National Inventory Report 2015 and 2016: Emission Inventories 1990-2014 - Submitted under the United Nations Framework Convention on Climate Change and the Kyoto Protocol. Technical report, DCE-Nationalt Center for Miljø og Energi.

Novan, K., 2015. Valuing the wind: Renewable energy policies and air pollution avoided. Am. Econ. J. Econ. Policy 7 (3), 291–326.

NREL, 2013. The Western Wind and Solar Integration Study, Phase 2. Technical report, National Renewable Energy Lab, Golden, CO (United States).

Oliveira, T., Varum, C., Botelho, A., 2019. Wind power and CO_2 emissions in the Irish market. Energy Econ. 80, 48–58.

O'Mahoney, A., Denny, E., Hobbs, B.F., O'Malley, M., 2018. The drivers of power system emissions: An econometric analysis of load, wind and forecast errors. Energy Syst. 9 (4), 853–872.

Pieralli, S., Ritter, M., Odening, M., 2015. Efficiency of wind power production and its determinants. Energy 90, 429–438.

Pindyck, R.S., 1999. The long-run evolutions of energy prices. Energy J. 20 (2).

Pindyck, R.S., 2001. The dynamics of commodity spot and futures markets: A primer. Energy J. 22 (3), 1–30.

SEAI, 2019. Energy in Ireland. Technical report, Sustainable Energy Authority of Ireland.

Siler-Evans, K., Azevedo, I.L., Morgan, M.G., 2012. Marginal emissions factors for the US electricity system. Environ. Sci. Technol. 46 (9), 4742–4748.

Stocker, T.F., Qin, D., Plattner, G.-K., Tignor, M., Allen, S.K., Boschung, J., Nauels, A., Xia, Y., Bex, V., Midgley, P.M., 2013. Climate Change 2013: The Physical Science Basis. Technical report, Contribution of Working Group I to the Fifth Assessment Report of the Intergovernmental Panel on Climate Change, Cambridge Univ. Press, Cambridge, UK, and New York.

Thomson, R.C., Harrison, G.P., Chick, J.P., 2017. Marginal greenhouse gas emissions displacement of wind power in Great Britain. Energy Policy 101, 201–210.

Valentino, L., Valenzuela, V., Botterud, A., Zhou, Z., Conzelmann, G., 2012. System-wide emissions implications of increased wind power penetration. Environ. Sci. Technol. 46 (7), 4200–4206.

Weldemichael, Y., Assefa, G., 2016. Assessing the energy production and GHG (greenhouse gas) emissions mitigation potential of biomass resources for Alberta. J. Clean. Prod. 112, 4257–4264.

Wheatley, J., 2013. Quantifying CO_2 savings from wind power. Energy Policy 63, 89–96.